

Strongly interacting trapped one-dimensional quantum gases: an exact solution

A. Minguzzi^{1, a)} and P. Vignolo^{2, b)}

¹⁾*Univ. Grenoble-Alpes, CNRS, LPMMC, 38000 Grenoble, France*

²⁾*Univ. Côte d'Azur, CNRS, InPhyNi, 06560 Valbonne, France*

(Dated: 10 January 2022)

Quantum correlations can be used as a resource for quantum computing, eg for quantum state manipulation, and for quantum sensing, eg for creating non-classical states which allow to achieve the quantum advantage regime. This review collects the predictions coming from a family of exact solutions which allows to describe the many-body wavefunction of strongly correlated quantum fluids confined by a tight waveguide and subjected to any form of longitudinal confinement. It directly describes the experiments with trapped ultracold atoms where the strongly correlated regime in one dimension has been achieved. The exact solution applies to bosons, fermions and mixtures. It allows to obtain experimental observables such as the density profiles and momentum distribution at all momentum scales, beyond the Luttinger liquid approach. It also predicts the exact quantum dynamics at all the times, including the small oscillations regime yielding the collective modes of the system and the large quench regime where the system parameters are changed considerably. The solution can be extended to describe finite-temperature conditions, spin and magnetization effects. The review illustrates the idea of the solution, presents the key theoretical achievements and the main experiments on strongly correlated one-dimensional quantum gases.

I. INTRODUCTION

Ultracold strongly correlated atomic gases are extremely rich and complex physical systems. One needs to take into account the quantum degeneracy, the particle indistinguishability and their symmetry properties under exchange, the effects of the spin degrees of freedom and of the interactions. The stronger is the interaction strength, the stronger are quantum correlations between the atoms and more difficult is to get an accurate description of the system, even numerically, and especially for the long-time dynamics. For these reasons, exact solutions for quantum systems are essential both for the deep understanding of fundamental physics and for the benchmark of classical and quantum simulators.

Exact solutions for one-dimensional (1D) homogeneous systems are well known in the literature. Celebrated examples are the cases of 1D bosons or fermions with contact interactions that are solvable by the Bethe Ansatz¹⁻³. Such solution assumes crucially that the system is homogeneous, as described by a ring or a hard-wall trap.

Several experiments on ultracold atoms, however, are performed in the presence of some type of external confinement, the most common being a harmonic trap and/or optical lattices. For confined 1D systems, integrability generally breaks down. A remarkable exception is the infinitely repulsive limit where the absence of a length scale associated to interactions allows to obtain an exact solution for any form of external confinement. This is the case, for instance, of the Tonks-Girardeau gas (TG), a gas of 1D bosons that can be mapped

onto a system of spinless non-interacting fermions⁴. Similarly, also multicomponent mixtures of bosons and fermions admit an exact solutions in the strongly repulsive limit.

This review is dedicated to such a category of exact solutions, for trapped bosons, fermions and mixtures at zero and finite temperature. It complements the existing reviews on general features of one-dimensional systems of ultracold atoms, specifically bosons^{5,6}, fermions⁷ and mixtures⁸. We will discuss how to build exact solutions in the infinite repulsive limit and in its proximity, and we will compare exact results with mean-field approaches and virial expansion in the high-temperature limit.

A. Experiments on 1D strongly correlated gases

The strategy to reach the strongly-correlated regime in 1D ultracold atomic gases consists in increasing the interaction strength with respect to the kinetic term: this can be realized in several ways: by means of Feshbach resonances⁹, by increasing the atomic effective mass with the presence of a lattice potential¹⁰, by decreasing the density, or by increasing the transverse confinement. The first experiments achieving the strongly correlated regime in 1D confinements have been realized in the early 2000's both for bosons^{9,10} and fermions¹¹. The signature of the approaching TG regime for bosons was observed in real space⁹ where fermionization shows up in the size cloud, and in momentum space¹⁰ where correlations manifest themselves (Fig. 1). In a subsequent experiment by Kinoshita et al.¹², the TG regime has been observed also in the strong decrease of two-body local correlations (see Fig. 2). Moreover, dynamical fermionization of bosons has been shown in the time evolution of the momentum distribution of an expanding cloud¹³. The control over experimental parameters is so accurate that it has been possible to make quantitative and stringent test of effective theories such as the Generalized Hydrodynamics¹⁴.

^{a)}Electronic mail: anna.minguzzi@lpmmc.cnrs.fr

^{b)}Electronic mail: patrizia.vignolo@inphynti.cnrs.fr

Fermionization of fermions, namely the fact that strongly repulsive multi-component fermions behave like a non-interacting spinless fermionic gas, has been proven in Ref. [15] for the case of a two-components mixture. Indeed the strongly correlated regime for ultracold gases can be obtained with multicomponent systems allowing s -wave scattering events at very low temperatures. Such mixtures offer the possibility to realize and study $SU(\kappa)$ systems (for instance $\kappa = 6$ in Ref. [16], see Fig. 3) for balanced or imbalanced mixtures¹⁷, paving the way for the study of quantum magnetism and BCS-like pairing. For instance, it has been proven that strongly-correlated fermions in a line are the experimental realization of a spin-chain Hamiltonian¹⁸. The 1D Cooper pair mechanism has also been studied¹⁹.

Fluctuations depend on the interaction regime. Number fluctuations have been studied in the crossover from weak to strong interactions in Ref. [20]. Typically, in ultracold atom experiments, the system is prepared in the ground state, but it has been shown that it is also possible to realize a highly excited state with attractive interactions, the super-TG gas²¹.

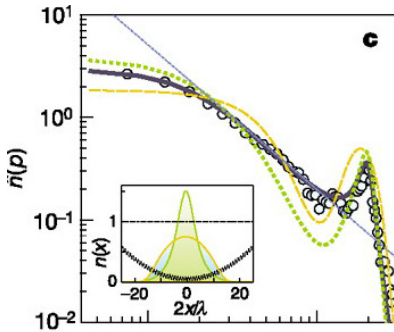


FIG. 1. From [10]. Experimental observation of the TG regime for quasi-1D bosons in optical lattices. The measured momentum distribution is compared to the one predicted for a TG gas on a lattice (solid violet line), finding a good agreement. The predictions for the momentum distribution of an ideal Fermi gas (yellow dashed lines) and of an ideal Bose gas (green dotted line) are also shown for comparison. Reprinted by permission from Springer Nature Customer Service Centre GmbH: Paredes *et al.*, Nature **429**, 277 (2004), copyright 2004 (<https://doi.org/10.1038/nature02530>).

Dynamical properties have then been explored in different setups. The dynamical structure factor has been studied in Ref. [23] and the non-equilibrium coherence dynamics in Ref. [24]. Ref. [25] has shown the absence of damping in a quasi-1D Bose gas driven out of equilibrium (see Fig. 4). This is the signature of the absence of collisions due to the reduced dimensionality: the oscillations have been shown to damp out if the dimensionality of the system is increased eg by allowing tunneling among the tubes of the 2D lattice.

Quantum dynamics of impurities in 1D Bose gases has been studied in Refs.[26],[27] and [28]. An impurity, dressed by the bosonic medium, feels an effective force which is smaller than the bare one²⁶, oscillates with an interacting-dependent amplitude²⁷ and makes Bloch oscillations in the absence of a lattice, the ranging of the bosons playing the role of the lattice²⁸.

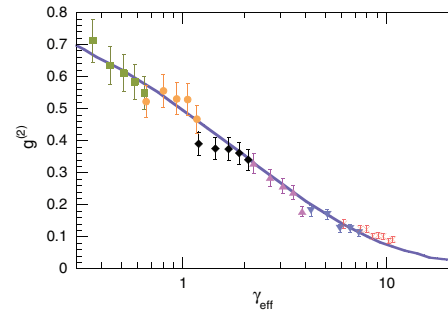


FIG. 2. From [12]. Measurement of the local pair correlations $g^{(2)}$ as a function of the coupling strength (data points) and 1D Bose gas theory from the Bethe Ansatz solution of the Lieb-Liniger model²² (solid line). The decrease of $g^{(2)}$ indicates approach to the strongly interacting regime; in the TG regime $g^{(2)}$ is predicted to vanish as for noninteracting fermions. Reprinted figure with permission from [12], <https://doi.org/10.1103/PhysRevLett.95.190406>. Copyright (2021) by the American Physical Society.

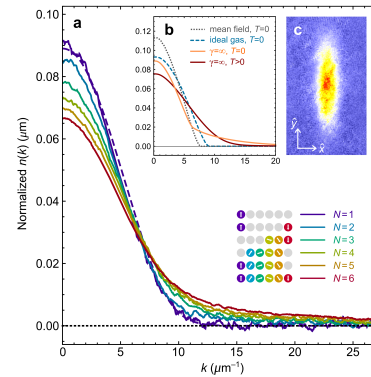


FIG. 3. From [16]. (a) Momentum distribution $n(k)$ measured with time-of-flight absorption imaging for different total number of atoms and the same atom number per spin component. (b) Theoretical $n(k)$ for the $N = 2$ system derived from different models. (c) Averaged absorption image. Reprinted by permission from Springer Nature Customer Service Centre GmbH: Pagano *et al.*, Nat. Phys. **10**, 198 (2014), copyright 2014 (<https://doi.org/10.1038/nphys2878>).

The list of experiments we have presented in this section is not exhaustive, but shows the increasing interest of the community for 1D strongly correlated systems and the increasing control of the experimental techniques in order to realize and manipulate such systems.

II. METHODS

A. Exact solution for zero-temperature bosons

We consider N bosons of mass m in one dimension, interacting with contact interactions $v(x-x') = g\delta(x-x')$ and subjected to a longitudinal confinement $V_{ext}(x)$. The effective interaction strength g for the one-dimensional problem can be expressed in terms of the three-dimensional interatomic s -

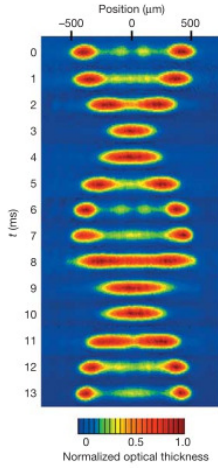


FIG. 4. From [25]. Absence of damping in a quasi-one-dimensional Bose gas driven out of equilibrium. Undamped oscillations are observed for an extremely long time, displaying the absence of collisional processes in quasi-1D gases. Reprinted by permission from Springer Nature Customer Service Centre GmbH: Kinoshita *et al.*, Nature **440**, 900 (2006), copyright 2006 (<https://doi.org/10.1038/nature04693>).

wave scattering length a_s and the typical scale for transverse confinement $a_{\perp} = \sqrt{\hbar/m\omega_{\perp}}$ which is assumed to be harmonic with frequency ω_{\perp} , leading to²⁹ $g = (4\hbar^2 a_s / ma_{\perp}^2)(1 - \alpha a_s / a_{1D})^{-1}$ with $\alpha = 1.4603\dots$. The Hamiltonian reads

$$H = \sum_{\ell=1}^N \left(-\frac{\hbar^2}{2m} \frac{\partial^2}{\partial x_{\ell}^2} + V_{ext}(x_{\ell}) \right) + g \sum_{1 \leq \ell < j \leq N} \delta(x_{\ell} - x_j). \quad (1)$$

This Hamiltonian corresponds to the Lieb-Liniger model³⁰. In absence of the external confinement, it can be solved by Bethe Ansatz for arbitrary interaction strength g . Here, we present an exact solution holding for any external confinement due to Girardeau⁴, valid in the limit of infinitely large repulsive interactions, ie for $g \rightarrow +\infty$, known as the Tonks-Girardeau (TG) limit.

The key idea of both the Bethe Ansatz and the Girardeau solution is to replace interactions by a cusp condition on the many-body wavefunction $\Psi(x_1, \dots, x_N)$,

$$\partial_x \Psi(x=0^+) - \partial_x \Psi(x=0^-) = \frac{mg}{\hbar^2} \Psi(x=0) \quad (2)$$

where $x = x_j - x_{\ell}$ for any pairs of particles $\{j, \ell\}$. Then, in the limit $g \rightarrow +\infty$ the many-body wavefunction must vanish at $x = 0$. In this regime there is no energy or length scale associated to interactions and the many-body wavefunction can be built by mapping onto a non-interacting spinless Fermi gas wavefunction $\Psi_A(x_1, \dots, x_N)$

$$\Psi_A(x_1, \dots, x_N) = \frac{1}{\sqrt{N!}} \det[\phi_j(x_{\ell})]_{j, \ell=1, \dots, N} \quad (3)$$

where the fermions are subjected to the same external confinement $V_{ext}(x)$, and the orbitals $\phi_j(x)$ are the solution of the

single-particle Schrödinger equation $\mathcal{H}_0 \phi_j = \varepsilon_j \phi_j$ with eigen-energies ε_j and $\mathcal{H}_0 = -\frac{\hbar^2}{2m} \frac{\partial^2}{\partial x^2} + V_{ext}(x)$. The exact many-body wavefunction for the TG gas then reads⁴

$$\Psi(x_1, \dots, x_N) = \prod_{j, \ell} \text{sign}(x_j - x_{\ell}) \Psi_A(x_1, \dots, x_N) \quad (4)$$

where the mapping function $\mathcal{A} = \prod_{j, \ell} \text{sign}(x_j - x_{\ell})$ ensures the bosonic symmetry under the exchange of two particles. In essence, interactions play the role of an effective Pauli principle and do not allow two particles to occupy the same spatial position or the same single-particle orbital. As we shall see below, there is a close connection among the Girardeau mapping and the Jordan-Wigner transformation³¹ introduced for lattice systems.

The choice of the orbitals in the fermionic wavefunction allows hence to describe an arbitrary bosonic state. The ground state of the bosonic problem corresponds to a filled Fermi sphere of the mapped Fermi gas, with corresponding ground-state energy $E_{GS} = \sum_{j=1}^N \varepsilon_j$, with $j = 1$ labelling the lowest-energy single-particle state.

The possibility of building a bosonic solution starting from a fermionic one is a signature of the statistical transmutation typical of one-dimensional systems. Extension to anyonic TG gases has also been studied³²⁻³⁵.

In the uniform system of length L with periodic boundary conditions corresponding to bosons on a ring, the ground-state many-body wavefunction reads^{4,36}

$$\Psi_{pbc}(x_1, \dots, x_N) = (L^N N!)^{-1/2} \prod_{1 \leq j < \ell \leq N} 2i \sin(\pi(|x_j - x_{\ell}|)/L). \quad (5)$$

Special care must be taken in this case depending on whether the number of bosons is even or odd: this is due to the fact that the mapping function \mathcal{A} is periodic for odd N and antiperiodic for even N : in the latter case one should use antiperiodic single-particle orbitals in order to ensure that the full many-body wavefunction is periodic.

Also in the case of a harmonic confinement $V_{ext}(x) = m\omega_0^2 x^2 / 2$ the wavefunction has an explicit solution. We have $\phi_j(x) = H_{j-1}(x/a_{ho}) e^{-x^2/2a_{ho}^2} / \sqrt{\pi 2^{j-1} (j-1)!}$, $\varepsilon_j = \hbar\omega_0(j - 1/2)$ with $a_{ho} = \sqrt{\hbar/m\omega_0}$ the harmonic oscillator length and H_j the Hermite polynomials. By using the fact that for Vandermonde determinants $\det p_{j-1}(x_k) = \prod_{1 \leq j < k \leq N} (x_k - x_j)$ for $p_j(x)$ polynomial of degree j with coefficient 1 in the x^j term, and the properties of the Hermite polynomials, the wavefunction can be explicitly written as³⁶⁻³⁸

$$\Psi_{ho}(x_1, \dots, x_N) = C_N \left[\prod_{1 \leq j < \ell \leq N} |x_j - x_{\ell}| \right] e^{-\sum_j (x_j/a_{ho})^2 / 2} \quad (6)$$

where $C_N = \sqrt{N!} [\prod_{m=0}^{N-1} 2^{-m} \sqrt{\pi m}]^{1/2}$ is a normalization constant.

Quite remarkably, the above equation (6) displays a striking connection to random matrix theory³⁹: $|\Psi_{ho}(x_1, \dots, x_N)|^2$ coincides with the joint distribution of the eigenvalues of a $N \times N$ matrix belonging to the Gaussian unitary ensemble (GUE). This also implies that the distribution of the position of the last fermion in the trap is of Tracy-Widom (TW-GUE) type.

The Girardeau solution can also be extended to a class of time-dependent problems, where the particles are subjected to

an arbitrary external time-dependent potential. Since the cusp condition must hold at all times, the solution by Girardeau can be extended to the time-dependent one⁴⁰

$$\Psi(x_1, \dots, x_N, t) = \Pi_{j,\ell} \text{sign}(x_j - x_\ell) \Psi_A(x_1, \dots, x_N, t) \quad (7)$$

where the fermionic wavefunction is built with time dependent single-particle orbitals corresponding to the solution of the Schrödinger equation $i\hbar\partial_t\phi_j = (-\hbar^2/2m) + V_{\text{ext}}(x, t)\phi_j$ and $\phi_j(x, 0)$ are the solution of the equilibrium Schrödinger equation in the initial potential $V_{\text{ext}}(x, 0)$. This approach allows to study a large class of problems where the initial Fermi sphere evolves under the effect of a time variation of the external trapping potential. As an example, we may cite the expansion and interference of a TG gas⁴⁰, the quench dynamics following a sudden change of the harmonic confinement⁴¹ as well as periodically driven systems⁴².

We also remark that the case of two hamonically trapped bosons has an exact solution for any value of the contact interaction strength g ⁴³. In such a case, $\Psi(x_1, x_2) = \phi_1(x_{CM})\psi_{\nu}(x_{rel})$, where $x_{CM} = (x_1 + x_2)/2$, $x_{rel} = x_1 - x_2$, and ν 's being the solutions of the transcendental equation

$$\frac{\Gamma(-\nu/2)}{\Gamma(-\nu/2 + 1/2)} = \sqrt{2} \frac{a_{1D}}{a_{ho}}. \quad (8)$$

The wavefunction solving the Schrödinger equation for the relative motion⁴³ reads

$$\psi_{\nu}(x_{rel}) = \frac{(\pi/2)^{1/4}}{\sqrt{a_{ho}}\sqrt{\mathcal{N}(\nu)}} \frac{2^{\nu/2}}{\Gamma(-\nu/2 + 1/2)} \Phi\left(-\frac{\nu}{2}, \frac{1}{2}, \frac{x_{rel}^2}{a_{ho}^2}\right) \quad (9)$$

where $\Gamma(u)$ is the gamma Euler function, Φ is the (Kummer) hypergeometric function, and

$$\mathcal{N}(\nu) = \Gamma(\nu + 1) \left\{ 1 + \frac{\sin(\pi\nu)}{2\pi} [\Psi(\frac{\nu}{2} + 1) - \Psi(\frac{\nu}{2} + \frac{1}{2})] \right\} \quad (10)$$

is a normalization factor involving the digamma function $\Psi(u) = \Gamma'(u)/\Gamma(u)$.

In all the above examples, we have described a continuous system. The analogue of the Girardeau solution can also be formulated on the lattice in the limit of hard-core bosons. In this case, specific commutation relations for the bosonic field operators a_j have to be imposed to ensure the impenetrability condition, namely $[a_i, a_j^\dagger] = \delta_{i,j}$ for $i \neq j$ and $\{a_i, a_i^\dagger\} = 1$, $a_i^2 = 0 = (a_i^\dagger)^2$. In the presence of an additional harmonic potential $V_j = V_2 x_j^2$ on the lattice sites $x_j = j\Delta x$, with Δx the lattice spacing, the corresponding Hamiltonian reads

$$H = -J \sum_j \left(a_j^\dagger a_{j+1} + H.c. \right) + V_2 \sum_j x_j^2 a_j^\dagger a_j, \quad (11)$$

where J is the tunnel amplitude among nearest lattice sites. The exact solution then follows from the Jordan-Wigner transformation

$$f_j^\dagger = a_j^\dagger \Pi_{\ell=1}^{j-1} e^{-i\pi f_\ell^\dagger f_\ell} \quad f_j = \Pi_{\ell=1}^{j-1} e^{i\pi f_\ell^\dagger f_\ell} a_j \quad (12)$$

which maps the hard-core bosons onto non-interacting fermions described by the fermionic field operators f_j . Exploiting the Wick's theorem, this allows to obtain the one-body density matrix of hard-core bosons in a closed form requiring only the knowledge of the single-particle eigenstates of the Hamiltonian H ⁴⁴ (see also [45] for an alternative procedure). The above method has also been extended to obtain finite-temperature properties⁴⁶ and the spectral function⁴⁷ of lattice bosons.

B. Specific focus on calculation of observables

Given the knowledge of the many-body wavefunction, still it is not always immediate to obtain physical observables. We provide in this section specific examples on how to compute the main observables accessible in ultracold-atom experiments.

1. Density profiles

The first observable accessible is the density profile that in terms of the bosonic creation and annihilation operators $\hat{\Psi}(x)$ and $\hat{\Psi}^\dagger(x)$ is defined as $n(x) = \langle \hat{\Psi}^\dagger(x) \hat{\Psi}(x) \rangle$. For the TG gas, by using the Bose-Fermi mapping, the density profile, as well as all other diagonal observables, is the same as the density profile for a spinless fermionic gas. If $\phi_j(x)$ are the single-particle orbitals for a non-interacting particles trapped in an external potential $V_{\text{ext}}(x)$, then the density profiles can be written

$$n(x) = \sum_{j=1}^N |\phi_j(x)|^2 = \sum_{j=1}^N \langle \phi_j | \delta(x - x_j) | \phi_j \rangle. \quad (13)$$

Several elementary methods may be employed to obtain the density profile for a small particle number. Here we describe a Green's function method specifically taylorred to address large systems. The key idea of the method is to express the δ function in Eq. (13) in terms of the imaginary part of the Green's function $G(x) = (x - \hat{x} + i\varepsilon)^{-1}$ for the position operator \hat{x} , getting the expression

$$n(x) = -\frac{1}{\pi} \lim_{\varepsilon \rightarrow 0^+} \text{Im} \sum_{j=1}^N \langle \phi_j | G(x) | \phi_j \rangle, \quad (14)$$

and by using the relation between the trace of a matrix and the determinant of its inverse

$$n(x) = -\frac{1}{\pi} \lim_{\varepsilon \rightarrow 0^+} \text{Im} \frac{\partial}{\partial \lambda} [\ln \det(x - \hat{x} + i\varepsilon + \lambda \mathbf{I})]_{\lambda=0} \quad (15)$$

where \mathbf{I} is a diagonal matrix with the first N diagonal elements equal to 1, and zero otherwise. Expressions (14) and (15) are particularly useful for the case of a harmonic trapping potential. Indeed, for such a system, the position operator expressed on Hamiltonian eigenstates basis is a tridiagonal matrix⁴⁸, whose non-zero elements takes the values $[\hat{x}]_{j,j+1} = \sqrt{j/2}$. This implies that all techniques developed to deal with 1D

tight-binding systems for the calculation of the density of states can be exploited for the calculation for the density profile of the harmonically trapped bosonic (fermionic) gas⁴⁸. In particular one can use the Kirkman and Pendry relation⁴⁹ in order to express the density profile as a function of only the $G_{1,N}(x)$ Green's function element⁵⁰. This is somehow equivalent to the fact that the total density can be expressed as a function of only two wavefunctions, ϕ_N and ϕ_{N-1} ⁵¹. Let us underline that the Green's function method sheds light on the quantum aspect of the system⁵⁰. Indeed one can observe that: (i) if one reduces the position operator to a $N \times N$ matrix, excluding all states that are not occupied by the fermions (at zero temperature), one obtains a density profile composed by N delta peaks: no exchange is possible among the particles; (ii) the Thomas-Fermi approximation, that leads to a smooth density profile where shell effects are not visible,

$$n_{\text{TF}}(x) = \sqrt{2N - x^2/a_{ho}^2}/(\pi a_{ho}) \quad (16)$$

corresponds to a single occupied state (the first) and to fix the "hopping" terms $[\hat{x}]_{j,j+1}$ to the value $\sqrt{N}/2$ for any j .

The Green's function method can be generalized to higher dimensions⁵². Alternatively it is also possible to express the exact density profile in term of a sum over Laguerre polynomials⁵³ or using random matrix theory^{39,54}. Three-dimensional shell effects have been numerically calculated in Refs. [55] and [56] and analytically in any dimension⁵⁷ to leading order in $1/N$.

At arbitrary interactions, the harmonically trapped system is not integrable. Still, at sufficiently large N , the density profile can be obtained using the local-density approximation. For one-dimensional bosons at finite interactions, by using the exact equation of state $\mu_{\text{hom}}[n]$ stemming from the Bethe Ansatz solution for the homogeneous system¹, one obtains the density profile using the implicit equation^{58,59}

$$\mu - V_{\text{ext}}(x) = \mu_{\text{hom}}[n(x)] \quad (17)$$

together with imposing the normalization condition $\int dx n(x) = N$ which fixes the value of the chemical potential μ of the trapped system. As the Thomas-Fermi approximation in the TG limit, the LDA neglects the shell structure on the density profile.

2. One-body density matrix

The reduced one body-density matrix embeds the first-order coherence properties of the system. It is defined as $\rho_1(x, y) = \langle \hat{\Psi}^\dagger(x) \hat{\Psi}(y) \rangle$. The one-body density matrix is a key quantity for bosonic systems since its behaviour at large distances characterizes the off-diagonal long-range order, and in particular allows to obtain the condensate density n_0 according to the Penrose and Onsager criterion, which for a homogeneous system reads $\rho_1(x, y) \rightarrow n_0$ for $|x - y| \rightarrow \infty$. In one dimensional systems there is no Bose-Einstein condensation, and the one-body density matrix decays as a power law for arbitrary (non-zero) interactions as predicted by the Luttinger

liquid theory⁶⁰ (see also⁶¹ for finite-size corrections). Finally, the one-body density matrix allows to obtain the momentum distribution of the gas by Fourier transform with respect to the relative coordinate,

$$n(k) = \int dx dy e^{ik(x-y)} \rho_1(x, y). \quad (18)$$

For the TG gas a closed-form expression for the one-body density matrix was provided by Lenard⁶². Its asymptotic behaviour in the homogeneous system has been studied with several techniques: at large distances as derived by the Lenard expansion⁶³⁻⁶⁵, using replica trick⁶⁶ and random matrix theory³⁶, as well as the short distances⁶⁷, where a general connection has been found between the coefficients of the one-body density matrix and the local two- and three-body correlators⁶⁸.

We detail here the calculation of the one-body density matrix for the TG gas, in a harmonic trap, following Ref. [36]. In first quantization, the one-body density matrix reads

$$\rho_1(x, y) = N \int dx_2, \dots, dx_N \Psi_{ho}^*(x, x_2, \dots, x_N) \Psi_{ho}(y, x_2, \dots, x_N). \quad (19)$$

Inserting the expression for the TG many-body wavefunction (4), in analogy to [62] it is possible to factor the many-body integrals into the determinant of one-body integrals, thus simplifying considerably the complexity of the calculation. The final result reads

$$\rho_1(x, y) = c_N^2 e^{-(x^2+y^2)/2a_{ho}^2} \det[b_{j,k}(x/a_{ho}, y/a_{ho})] \quad (20)$$

with

$$b_{j,k} = c_j c_k \int_{-\infty}^{\infty} dz e^{-z^2} (x-z)(y-z) z^{j+k-2} - 2 \text{sign}(x-y) \int_x^y dz e^{-z^2} (x-z)(y-z) z^{j+k-2} \quad (21)$$

and $c_j = [2^{j-1}/\sqrt{\pi}\Gamma(j)]^{1/2}$. The latter integral can be explicitly calculated in terms of the incomplete γ function and confluent hypergeometric functions³⁶. For large N , it can be shown that the one-body density matrix reduces to³⁶

$$\rho_1(x, y) \sim N^{1/2} \frac{[G(3/2)]^4 (1 - (x/R_{TF})^2)^{1/8} (1 - (y/R_{TF})^2)^{1/8}}{\pi |x/R_{TF} - y/R_{TF}|^{1/2}} \quad (22)$$

where $R_{TF} = \sqrt{2N}a_{ho}$ is the Thomas-Fermi radius and $G(z)$ is the Barnes G-function. A useful extension of Lenard's method allows to obtain the expression of the time-dependent one-body density matrix, $\rho_1(x, y, t) = \langle \Psi^\dagger(x, t) \Psi(y, t) \rangle$ with $\Psi(x, t) = e^{iHt} \Psi(x) e^{-iHt}$, whose dynamical evolution could be due e.g. to a quench of the system parameters. In such a case, using the time-dependent Bose-Fermi mapping and exploiting the properties of the determinants one has⁶⁹

$$\rho_1(x, y, t) = \sum_{j, \ell=1}^N \phi_j^*(x, t) A_{j\ell}(x, y, t) \phi_\ell(y, t), \quad (23)$$

where the $N \times N$ matrix $\mathbf{A}(x, y, t)$ is given by $\mathbf{A}(x, y, t) = (\mathbf{P}^{-1})^T \det \mathbf{P}$ and $P_{j\ell}(x, y, t) = \delta_{j\ell} - 2 \text{sgn}(x -$

$y) \int_x^y dx' \phi_j^*(x', t) \phi_\ell(x', t)$. This approach allows for a very efficient and exact (up to numerical accuracy) calculation of the time evolution of the one-body density matrix. A finite-temperature extension of the above result has been demonstrated using Fredholm determinants approach⁷⁰, valid each time the wavefunctions vanish at the boundaries of the system (eg for harmonically trapped or hard-wall potentials).

3. Higher order correlators

As we have seen in the previous section, the one-body density matrix provides the momentum distribution that, together with the density profile, represents one of the main observable easily accessible in ultracold atoms. Spatial and momentum fluctuations around the average are more difficult to be detected⁷¹, but they can lead the most interesting signal as known in phase transitions or quantum optics. Actually there is a particular interest in studying higher momentum occupation number, like the momentum distribution variance $\sigma_p^2 = \langle N_p^2 \rangle - \langle N_p \rangle^2$ and covariance $\langle N_p N_q \rangle$ ⁷²⁻⁷⁷, or the full counting statistics^{76,77}.

The momentum distribution variance and covariance are obtained by the Fourier transform of the two-body density matrix, that in first quantization reads

$$\rho_2(x_1, x_2; y_1, y_2) = \int dx_3 \cdots \int dx_N \Psi(x_1, x_2, x_3, \dots, x_N) \Psi^*(y_1, y_2, x_3, \dots, x_N). \quad (24)$$

Indeed

$$\langle N_p N_q \rangle = \int dx_1 \int dx_2 \int dy_1 \int dy_2 e^{ip(y_1 - x_1)} e^{iq(y_2 - x_2)} \rho_2(x_1, x_2; y_1, y_2). \quad (25)$$

For the homogeneous TG gas it has been found that, at any momentum p , with $p \neq 0$ ^{76,77},

$$\langle N_p N_q \rangle = (1 + \delta_{p,q}) \langle N_p \rangle \langle N_q \rangle, \quad (26)$$

and the full counting statistics of N_p is exponential. The fact that there is no correlations if $p \neq q$ is very different from the weakly interacting case where pairs with opposite momenta are expected by the Bogolubov theory. At $p = q = 0$ the signature of quasi-long-range coherence is a decreasing function of fluctuations. In this case, it has been found that⁷⁷ $\langle N_0^2 \rangle = 1.33 \langle N_0 \rangle^2$ and the full quantum statistics is neither exponential nor Gumbel as predicted in the weakly interacting system⁷⁶, but seems to be in good agreement with a positive-Gaussian distribution⁷⁷. In the trap system, it has been shown that non trivial correlations, including negative correlations appear for momenta smaller or of the order of the inverse radius of the gas⁷⁸.

4. Dynamical structure factor and spectral function

The time-dependent Bose-Fermi mapping allows to obtain in an exact way dynamical correlation functions, as the dy-

namical structure factor $S(k, \omega)$, and the spectral function $A(k, \omega)$.

Dynamical structure factor. The dynamical structure factor is defined as the space-time Fourier transform of the connected density-density correlations $S(k, \omega) = \mathcal{F} \langle n(x, t) n(y, 0) \rangle_c$, with $\langle AB \rangle_c = \langle AB \rangle - \langle A \rangle \langle B \rangle$ and $\langle \dots \rangle$ denotes the quantum average on the state of the system. It yields information on the spectrum of the system collective excitations, ie the response of the fluid upon the transfer of an energy $\hbar\omega$ and a momentum $\hbar k$. This quantity is accessible in quantum gases experiments via Bragg scattering techniques⁷⁹⁻⁸¹.

Since it involves only the density operators $n(x, t)$, the dynamical structure factor of the TG gas coincides with the one of a noninteracting Fermi gas. In the general case of a gas under external confinement, it reads

$$S(k, \omega) = 2\pi \sum_{i,j} \left| \int dx e^{-ikx} \phi_i^*(x) \phi_j(x) \right|^2 \times f(\varepsilon_i) [1 - f(\varepsilon_j)] \delta(\omega - \omega_{ij}). \quad (27)$$

with $\omega_{ij} = \varepsilon_j - \varepsilon_i$ and $\phi_j(x)$ the single particle orbitals solution of the equilibrium Schrödinger problem. In the case of harmonic external potential we have⁷⁹

$$\mathcal{S}(k, h) = 2\pi e^{-k^2/2} \sum_{i=\max\{N-h, 0\}}^{N-1} \frac{i!}{(i+h)!} \left(\frac{k^2}{2} \right)^h \left[L_i^h(k^2/2) \right]^2. \quad (28)$$

Here h is an integer corresponding to a single-atom excitation of h quanta of the harmonic oscillator and $L_i^h(x)$ is the i^{th} generalized Laguerre polynomial of parameter h .

It is useful to mention that a local-density approximation for the dynamical structure factor yields a good approximation if $\omega \gg \omega_0$. The LDA reads $S_{LDA}(k, \omega) = \int dx n(x) S_{hom}(k, \omega; \mu[n(x)])$, with $\mu[n]$ being the equation of state, which in the TG gas reads $\mu[n] = \pi^2 n^2 / 2m$, and $n(x)$ being the density profile of the gas.

Spectral function The spectral function is defined as $A(k, \omega) = -\frac{1}{\pi} \text{Im} G^R(k, \omega)$ where the retarded Green's function $G^R(k, \omega)$ is the Fourier transform of $G^R(x, t; y, t') = \theta(t - t') [G^>(x, t; y, t') - G^<(x, t; y, t')]$ with $G^<(x, t; y, t') = -i \langle \hat{\Psi}^\dagger(y, t') \hat{\Psi}(x, t) \rangle$, and $G^>(x, t; y, t') = -i \langle \hat{\Psi}(x, t) \hat{\Psi}^\dagger(y, t') \rangle$ being the lesser and greater Green's functions. The spectral function contains the information on the response of the system when a particle is extracted or added to the system with wavevector $\hbar k$ and energy $\hbar\omega$. At difference from the dynamical structure factor, this quantity has bosonic character, ie it is very different from its fermionic counterpart.

Thanks to the knowledge of the many-body wavefunction, it is possible to provide a closed, exact expression for the spectral function of the TG gas in arbitrary external potential⁴⁷. To give an idea of the calculation, we provide some details for the case of the lesser Green's function. We start from its definition,

$$\begin{aligned} iG^<(x, t, y, t')_\eta &= \langle \hat{\Psi}^\dagger(y, t') \hat{\Psi}(x, t) \rangle_\eta \\ &= \left\langle e^{iHt'} \hat{\Psi}^\dagger(y) e^{-iHt'} e^{iHt} \hat{\Psi}(x) e^{-iHt} \right\rangle_\eta \end{aligned} \quad (29)$$

where $\langle \dots \rangle_\eta$ indicates the expectation value over the many-body state $|\eta\rangle$ with $\eta = \{\eta_1, \dots, \eta_N\}$ single-particle quantum numbers, H is the many-body Hamiltonian and $\hat{\psi}(x)$, $\hat{\psi}^\dagger(x)$ are bosonic field operators, satisfying the commutation relations $[\hat{\psi}(x), \hat{\psi}^\dagger(y)] = \delta(x-y)$. Using the completeness relation and setting $X = x_2 \dots x_N$, $Y = y_2 \dots y_N$, the lesser Green's function in first quantization reads

$$iG^<(x, t, y, t')_\eta = \frac{e^{iE_\eta(t-t')}}{(N-1)!^2} \sum_n e^{-iE_n(t-t')} \int dY \Psi_n^*(y, Y) \Psi_n(Y) \times \int dX \Psi_n^*(X) \Psi_n(x, X).$$

Using the exact expression for the many-body wavefunction of the state Ψ_η and for the excited states Ψ_n belonging to the $N-1$ sector of the Hilbert space, we obtain the expression for the lesser Green's function of a TG gas:

$$iG^<(x, t, y, t') = \text{Det}[\mathbf{P}(x, t) \mathbf{P}(y, t') |_{\eta\eta}] a^<(x, t, y, t') \quad (30)$$

where

$$a^<(x, t, y, t') = \vec{\phi}(x, t)_\eta^T ([\mathbf{P}(x, t) \mathbf{P}(y, t')]^{-1})^T |_{\eta\eta} \vec{\phi}^*(y, t')_\eta, \quad (31)$$

with $\mathbf{P}_{lm}(x, t) = \int_{-\infty}^{\infty} \text{sign}(x - \bar{x}) \phi_l(\bar{x}, t) \phi_m^*(\bar{x}, t) d\bar{x} = \delta_{l,m} - 2 \int_{-\infty}^{\infty} e^{-u(\epsilon_l - \epsilon_m)} \phi_l(\bar{x}) \phi_m^*(\bar{x}) d\bar{x}$ and $\vec{\phi}(x, t) = [\phi_1(x, t), \dots, \phi_M(x, t)]^T$. As a comparison, the fermionic Green's function reads $G_F^<(x, t, y, t') = i \sum_\eta e^{-iE_\eta(t-t')} \phi_j^*(y) \phi_j(x)$, ie it is diagonal in the particle space basis. We see then explicitly that the spectral function is a bosonic observable, ie does not coincide with the corresponding observable in the mapped Fermi gas. Notice that the above result recovers Pezer and Buljan result for the equal-time correlator⁶⁹. Equation (30) hence allows for an efficient numerical implementation. A similar derivation can be done for $G^>(x, t, y, t')$. The above expression is fully general, ie it applies to any state η . Of special interest is the case when η is the ground state, hence allowing to obtain the zero-temperature expression for $A(k, \omega)$.

C. Multicomponent mixtures of bosons and fermions

We consider a mixture of $N_B = N_1^B + \dots + N_b^B$ bosons and $N_F = N_1^F + \dots + N_f^F$ fermions, with $N = N_B + N_F$, divided in b and f spin components⁸². We assume a supersymmetric model where all particles have same mass m , all particles experience the same trapping potential $V_{ext}(x)$, and the interaction between particles $V_{int}(x, y) = g\delta(x-y)$ does not depend on the spin. This is compatible with the fact that fermions with the same spin do not interact since the wavefunction being antisymmetric for exchange of two identical fermions, the interaction term does not play any role.

The positions of the particles are given by the coordinates $x_1^{B,1}, \dots, x_{N_B}^{B,b}, x_{N_B+1}^{F,1}, \dots, x_N^{F,f}$. For the sake of simplicity of notations, in the following, if not needed, we will omit the exponents specifying the type and the spin of the particles. Using

this notation, the Hamiltonian describing the system is formally the same as the one for the bosons (1). As a consequence of the cusp condition (2) that holds for the mixture too, in the limit $g \rightarrow +\infty$ the many-body wavefunction vanishes whenever $x_i = x_j$. Thus it can be written^{83,84}

$$\Psi(x_1, \dots, x_N) = \sum_{P \in S_N} a_P \theta_P(x_1, \dots, x_N) \Psi_A(x_1, \dots, x_N) \quad (32)$$

where S_N is the permutation group of N elements, $\theta_P(x_1, \dots, x_N)$ is equal to 1 in the coordinate sector $x_{P(1)} < \dots < x_{P(N)}$, and Ψ_A is the fully antisymmetric fermionic wavefunction (3). The coefficients a_P in Eq. (32) for the case of the exchange of identical fermions are equal to 1, and for the case of the exchange of identical bosons are equal to -1. Thus the number of independent coefficients is reduced to

$$D_{N,b+f} = \frac{N!}{N_1! \dots N_{b+f}!}. \quad (33)$$

We can thus reduce the dimensionality of our system from $N!$ to $D_{N,b+f}$ by regrouping the sectors that are equal *modulo* permutations of identical particles. We call this basis the snippet basis^{85,86}.

In order to find all the other coefficients a_P of the ground-state wavefunction we use a variational approach⁸⁷, by calculating the energy at the first order with respect the small parameter $1/g$ (for a similar treatment on the lattice case see⁸⁸) and by minimizing it in the limit $g \rightarrow \infty$,

$$E_g \simeq E_{g \rightarrow \infty} + \frac{1}{g} [\partial_{1/g} E]_{1/g \rightarrow \infty} = E_{g \rightarrow \infty} - \frac{1}{g} K. \quad (34)$$

Remark that this corresponds to maximize K that, as we will see in Sec. II E is proportional to the Tan's contact⁸⁹. The procedure is the following. One write $K(a_P)$ by exploiting the cusp condition (2),

$$K(a_P) = \sum_{P, Q \in S_N} (a_P - a_Q)^2 \alpha_{P, Q}, \quad (35)$$

where

$$\alpha_{P, Q} = \int dx_1, \dots, dx_N \theta_{\text{Id}}(x_1, \dots, x_N) \delta(x_k - x_{k+1}) [\partial \Psi_A / \partial x_k]^2 \equiv \alpha_k \quad (36)$$

if P and Q are equal up to a transposition of two consecutive distinguishable particles or indistinguishable bosons. Then one imposes the stationarity of $K(a_P)$, taking into account the normalization condition $\sum_P a_P^2 = 1$, by introducing the Lagrange multiplier λ

$$\partial_{a_P} [K(a_P) + \lambda \sum_P a_P^2] = 0. \quad (37)$$

This leads to the diagonalization problem

$$\tilde{K} \mathbf{a}_{\text{snip}} = \lambda \mathbf{a}_{\text{snip}}, \quad (38)$$

where \mathbf{a}_{snip} is the vector of the $D_{N,b+f}$ independent a_i coefficients, and \tilde{K} is a $D_{N,b+f} \times D_{N,b+f}$ matrix defined in the snippet basis by

$$\tilde{K}_{i,j} = \begin{cases} -\alpha_{i,j} & \text{if } i \neq j \\ \sum_{d,k \neq i} \alpha_{i,k} + 2\sum_{b,k \neq i} \alpha_{i,k} & \text{if } i = j \end{cases} \quad (39)$$

where the index d means that the sum has to be taken over snippets k that transpose distinguishable particles as compared to snippet i , while b means that the sum is taken over sectors that transpose identical bosons. The a_p 's corresponding to the highest eigenvalue of \tilde{K} yield the ground state of the system. The eigenstates corresponding to the other eigenvalues give access to the excited states belonging to the same $D_{N,b+f}$ degenerate manifold at $g \rightarrow \infty$.

Our solution generalizes the one for the homogeneous system to arbitrary external potential in the hard-core limit $g \rightarrow \infty$. Indeed, in the homogeneous case (periodic boundary conditions or hard walls) the Bethe Ansatz provides an exact expression for the many-body wavefunction of multicomponent supersymmetric mixtures at arbitrary interaction g (see eg⁹⁰ for a review). Let us point out that the case of few trapped SU(2) fermions, with finite interactions, has been tackled in [91] and [92].

Finally, for fermionic SU(κ) mixtures, with κ the number of components, the above approach has been extended to time-dependent problems⁹³. In this case the solution is exact to order $1/g$, and is based on the mapping onto a Heisenberg SU(κ) Hamiltonian^{84,94,95} on a lattice of N sites, where $N = N_1 + \dots + N_\kappa$ is the total number of fermions:

$$H_S = (E_0 - \sum_i^{N-1} J_i) + \sum_{i=1}^{N-1} J_i P_{i,i+1}. \quad (40)$$

Here $P_{i,i+1}$ is the permutation operator among the particle i and $i+1$, E_0 is the Fermi energy for the mixture, and $J_i = \alpha_i/g$ is a site-dependent hopping amplitude related to the overlaps α_i given in Eq. (36) above. An accurate expression for the exchange constants at large N is given by⁸⁴ (see also [96] and [97])

$$J_i = \frac{\hbar^4 \pi^2 n_{TF}^3(x_i)}{3m^2 g} \quad (41)$$

where n_{TF} is the Thomas-Fermi profile (16) and x_i is the center of mass of the i -th and $(i+1)$ -th particle. The many-body wavefunction is then still described by Eq. (32), but with time-dependent coefficients $a_p(t)$ and $\alpha_i(t)$. The time evolution of the coefficients a_p is determined by the Heisenberg Hamiltonian (40). The time dependence of the coefficients α_i is due to the time variations of the external trapping potential⁹³. Purely spin dynamics, i.e. with α_i constant in time, is realized by a suitable choice of the dynamical excitation protocol⁹⁸.

1. Symmetry considerations

Being the Hamiltonian (1) invariant with respect to permutation symmetry, its eigenstates can be labelled via the Young

diagrams corresponding to the irreducible representations of the permutation group S_N ⁹⁹. As we shall see below, symmetry properties emerge in physical observables, e.g. in the momentum distribution tails.

In order to obtain the symmetry associated with a given wave function $\Psi(x_1, \dots, x_N)$ belonging to the degenerate manifold, we define a set of $D_{N,b+f} \times D_{N,b+f}$ matrices, the p -cycle class-sums operators^{99,100}, whose eigenvalues are directly connected to the irreducible representations of S_N , and thus to the Young tableaux. The p -cycle class-sum operator $\Gamma^{(p)}$ is the sum of the permutation of p elements in a cyclic way. For instance, the structure of $\Gamma^{(2)} = \sum_{i < j} (i, j)$ on the snippet basis is the following:

- the diagonal elements $[\Gamma^{(2)}]_{A,A}$ are equal to $b_{N_b > 1} - f_{N_f > 1}$, $b_{N_b > 1}$ and $f_{N_f > 1}$ being the number of bosonic and fermionic components with a number of particles per component greater than one;
- the off-diagonal elements $[\Gamma^{(2)}]_{A,B}$ are equal to -1 (+1) if snippets A and B differ by the permutation of two distinguishable fermions (bosons);
- the off-diagonal elements $[\Gamma^{(2)}]_{A,B}$ are equal to $-1^{\mathcal{N}_f}$ if snippets A and B differ by the permutation of a boson with a fermion with in between \mathcal{N}_f fermions;
- the other off-diagonal elements are zero.

For the case of 4 particles p_i , with two particles per component i , $D_{N,b+f} = 6$: $p_1 p_1 p_2 p_2$, $p_1 p_2 p_1 p_2$, $p_1 p_2 p_2 p_1$, $p_2 p_1 p_1 p_2$, $p_2 p_1 p_2 p_1$, $p_2 p_2 p_1 p_1$. If $f = 2$ and $b = 0$,

$$\Gamma_{N=4, f=2, b=0}^{(2)} = \begin{pmatrix} -2 & 1 & -1 & -1 & 1 & 0 \\ 1 & -2 & 1 & 1 & 0 & 1 \\ -1 & 1 & -2 & 0 & 1 & -1 \\ -1 & 1 & 0 & -2 & 1 & -1 \\ 1 & 0 & 1 & 1 & -2 & 1 \\ 0 & 1 & -1 & -1 & 1 & -2 \end{pmatrix} \quad (42)$$

with eigenvalues $\gamma^{(2)} = \{-6, -2, -2, -2, 0, 0\}$. These $\gamma^{(2)}$'s

correspond to the Young tableaux $(1,1,1,1) = \begin{array}{|c|c|c|c|} \hline \square & \square & \square & \square \\ \hline \end{array}$, $(2,1,1) = \begin{array}{|c|c|c|} \hline \square & \square & \square \\ \hline \square & & \\ \hline \end{array}$, and $(2,2) = \begin{array}{|c|c|} \hline \square & \square \\ \hline \square & \square \\ \hline \end{array}$, whose dimensions d (1,3 and 2 respectively) is given by the Hook formula

$$d = \frac{N!}{\prod_{(i,j)} h(i,j)} \quad (43)$$

where $h(i,j)$ is equal to the number of cells below the box (i,j) + the number of cells at the right of the box $(i,j) + 1$. Indeed the relation between the $\gamma^{(2)}$'s and a Young tableaux with a number of boxes λ_i at line i is

$$\gamma^{(2)} = \frac{1}{2} \sum_i [\lambda_i (\lambda_i - 2i + 1)]. \quad (44)$$

For the case of $f = 0$ and $b = 2$, i.e. a two-component Bose-Bose mixture, $\Gamma_{N=4, f=0, b=2}^{(2)} = -\Gamma_{N=4, f=2, b=0}^{(2)}$. Its eigenvalues

$\gamma^{(2)} = \{6, 2, 2, 2, 0, 0\}$ correspond to the Young tableaux (4)= $\square\square\square\square$, (3,1)= $\square\square\square$, and (2,2)= $\square\square$, again with dimensions 1, 3 and 2.

For the case $f = 1$ and $b = 1$ ⁸⁶, i.e. a Bose-Fermi mixture,

$$\Gamma_{N=4, f=1, b=1}^{(2)} = \begin{pmatrix} 0 & -1 & -1 & 1 & 1 & 0 \\ -1 & 0 & -1 & -1 & 0 & 1 \\ -1 & -1 & 0 & 0 & -1 & -1 \\ 1 & -1 & 0 & 0 & -1 & 1 \\ 1 & 0 & -1 & -1 & 0 & -1 \\ 0 & 1 & -1 & 1 & -1 & 0 \end{pmatrix}. \quad (45)$$

The eigenvalues $\gamma^{(2)} = \{-2, -2, -2, 2, 2, 2\}$ correspond respectively to (2,1,1)= $\square\square$ and (3,1)= $\square\square\square$, each one with dimension 3. As we will see in the Sec. III, the ground state is always given by the most symmetric configuration (corresponding to the highest $\gamma^{(2)}$).

Remark that for $N > 5$ the class-sum operator $\Gamma^{(2)}$ is not sufficient to label the Young tableaux and thus the symmetry of the system, since different diagrams can have the same eigenvalue $\gamma^{(2)}$. In this case one needs to look at the other sum-class operators $\Gamma^{(p)}$, with $p > 2$ in order to uniquely identify the symmetry of a state. The general relation between the eigenvalues $\gamma^{(p)}$ and the Young tableaux with n lines reads^{82,101}

$$\gamma^{(p)} = \frac{1}{p} \sum_{i=1}^n \mu_i (\mu_i - 1) \dots (\mu_i - p + 1) \prod_{j \neq i} \frac{\mu_i - \mu_j - p}{\mu_i - \mu_j} \quad (46)$$

where $\mu_i = \lambda_i - i + n$.

D. Finite temperature bosons and fermions

1. Thermal Bose-Fermi mapping and diagonal observables

The exact solution in the limit of infinite interactions both for TG bosons and multi-component fermions can be extended at finite temperature.

We detail first the bosonic case. The key idea is that the Bose-Fermi mapping holds for any many-body energy eigenvalue, hence we can build a thermal density matrix for the TG gas in terms of the one of a Fermi gas. Writing the bosonic thermal density matrix as $\hat{\rho}_B = \sum_{N, \alpha} w_{N, \alpha} |\Psi_{BN\alpha}\rangle \langle \Psi_{BN\alpha}|$, with $w_{N, \alpha} = \exp[-\beta(E_{N, \alpha} - \mu N)]/Z$, α the state quantum number, $\beta = 1/k_B T$, μ the chemical potential and $Z = \sum_{N, \alpha} w_{N, \alpha}$, the expectation value of any observable \hat{O} is given by $\langle \hat{O} \rangle = \sum_{N, \alpha} w_{N, \alpha} \langle \Psi_{BN\alpha} | \hat{O} | \Psi_{BN\alpha} \rangle$. The Bose-Fermi mapping for a given energy eigenstate $|\Psi_{B\alpha}\rangle$ states that it can be written in terms of the one of a noninteracting Fermi gas by the mapping operator \hat{A} , such that $|\Psi_{BN\alpha}\rangle = \hat{A} |\Psi_{FN\alpha}\rangle$. In coordinate representation, for a N -particle state $|\Psi_{BN\alpha}\rangle$ the many-body wavefunction reads

$$\Psi_{N\alpha}(x_1 \dots x_N) = \prod_{1 \leq j < \ell \leq N} \text{sign}(x_j - x_\ell) \Psi_{N\alpha}^F(x_1, x_2, \dots, x_N). \quad (47)$$

where $\alpha = \{v_1, \dots, v_N\}$ is the set of single-particle quantum numbers, $\Psi_{N\alpha}^F(x_1, x_2, \dots, x_N) = \frac{1}{\sqrt{N!}} \det[\phi_{v_j}(x_k)]$ is the fermionic wavefunction constructed with the single particle orbitals $\phi_{v_j}(x)$ corresponding single-particle energies ε_{v_j} , allowing to obtain the energy $E_{N\alpha} = \sum_{j=1}^N \varepsilon_{v_j}$. The statistical Bose-Fermi mapping reads¹⁰²

$$\langle \hat{O} \rangle = \sum_{\alpha} w_{\alpha} \langle \Psi_{F\alpha} | A^{-1} \hat{O} A | \Psi_{F\alpha} \rangle. \quad (48)$$

Of specific interest are the observables that commute with the mapping operator \hat{A} , as the density and particle current operators. In this case their expectation value coincides with the fermionic one. For the particle density one has

$$n(x) = \frac{1}{Z} \sum_{N, \alpha} e^{-\beta(E_{N, \alpha} - \mu N)} n_{N\alpha}(x) \quad (49)$$

with $n_{N\alpha}(x) = \sum_{j=1}^N |\phi_{v_j}(x)|^2$ which leads to

$$n(x) = \sum_{j=1}^{\infty} f(\varepsilon_j) |\phi_j(x)|^2 \quad (50)$$

with $f(\varepsilon_j) = 1/(e^{\beta(\varepsilon_j - \mu)} + 1)$ the Fermi occupation numbers. The chemical potential at temperature T and average particle number N is obtained by setting $N = \sum_{j=1}^{\infty} f(\varepsilon_j)$. An analytical expression for the thermal particle density at large N is given by⁵⁴

$$n(x) = -\frac{1}{a_{ho} \sqrt{N}} \sqrt{\frac{k_B T}{2\pi N \hbar \omega_0}} \text{Li}_{1/2} \left(-\left(e^{\frac{N \hbar \omega}{k_B T}} - 1 \right) \exp \left[-\frac{m \omega_0^2 x^2}{2k_B T} \right] \right). \quad (51)$$

Similarly, the particle current density of a TG gas at finite temperature coincides with the one of a Fermi gas and reads

$$j(x) = \frac{i\hbar}{2m} \sum_{j=1}^{\infty} f(\varepsilon_j) [\phi_j^*(x) \partial_x \phi_j(x) - (\partial_x \phi_j^*(x)) \phi_j(x)]. \quad (52)$$

Notice that all the above expressions can be used also to describe the time evolution of an initial thermal state, the time dependence being included in the evolution of the single-particle orbitals $\phi_j(x, t)$ ¹⁰²⁻¹⁰⁶.

The same results hold for fermionized fermions and Bose-Fermi mixtures by a straightforward generalization of the previous mapping¹⁰⁷.

2. Finite temperature one-body density matrix

The Bose-Fermi mapping (47) allows to construct the thermal average for the TG one-body density matrix :

$$\rho_{1B}(x, y) = \sum_{N, \alpha} P_{N, \alpha} N \int_I dx_2, \dots, dx_N \times \Psi_{N, \alpha}(x, x_2, \dots, x_N) \Psi_{N, \alpha}^*(y, x_2, \dots, x_N). \quad (53)$$

Here $I = (-\infty, \infty)$ is the spatial integration domain, $P_{N,\alpha} = e^{-\beta(E_{N,\alpha} - \mu N)} / Z$ is the thermal distribution function, $Z = \sum_{N,\alpha} e^{-\beta(E_{N,\alpha} - \mu N)}$ the partition function for the TG gas with $E_{N,\alpha} = \sum_{j=1}^N \varepsilon_{v_j}$, $\beta = 1/k_B T$, and μ the chemical potential. Equation (53) can be simplified as illustrated in an early work by Lenard¹⁰⁸. The resulting expression reads¹⁰⁹

$$\rho_{1B}(x, y) = \sum_{j=0}^{\infty} \frac{(-2)^j}{j!} (\text{sign}(x-y))^j \rho_{1B}^{(j)}(x, y) \quad (54)$$

where we have defined

$$\rho_{1B}^{(j)}(x, y) = \int_x^y dx_2 \dots dx_{j+1} \det[\rho_{1F}(x_i, x_\ell)]_{i,\ell=1,j+1}, \quad (55)$$

$\rho_{1F}(x, y) = \sum_{j=1}^N f_j \phi_j(x) \phi_j^*(y)$ being the *fermionic* one-body density matrix, $f_j = 1/[e^{\beta(\varepsilon_j - \mu)} + 1]$ the Fermi occupation factor of a single-particle energy level, and in the above determinant one has to take $x_i = x$ for $i = 1$ and $x_\ell = y$ for $\ell = 1$. Using the definition of the fermionic one-body density matrix, the j -th term of the one-body density matrix is given by

$$\rho_{1B}^{(j)}(x, y) = \sum_{v_1 \dots v_{j+1}} f_{v_1} \dots f_{v_{j+1}} \sum_{P \in \mathcal{S}_{j+1}} (-1)^P \phi_{v_1}(x) \phi_{v_{P(1)}}(y) \prod_{\ell=2}^{j+1} \int_x^y dx_\ell \phi_{v_\ell}(x_\ell) \phi_{v_{P(\ell)}}^*(x_\ell). \quad (56)$$

This can be finally casted onto the compact form^{69,110,111}

$$\rho_{1B}^{(j)}(x, y) = \sum_{v_1 \dots v_{j+1}} f_{v_1} \dots f_{v_{j+1}} \sum_{k=1}^{j+1} \phi_{v_1}(x) A_{v_1 v_k}(x, y) \phi_{v_k}^*(y) \quad (57)$$

where $A_{v_1 v_k}(x, y)$ can be expressed as functions of special functions for the case of a harmonically trapped gas¹⁰⁹.

Another strategy to reduce the calculation of the thermal one-body density matrix to a simple double sum has been found by the authors of Ref. [70]. Indeed it can be shown that one can write

$$\rho_{1B}(x, y) = \sum_{i,j=0}^{\infty} \sqrt{f_i} \phi_i(x) Q_{ij} \sqrt{f_j} \phi_j^*(y) \quad (58)$$

where Q_{ij} are the matrix elements of the operator

$$Q(x, y) = (P^{-1})^T \det P \quad (59)$$

with

$$P_{ij}(x, y) = \delta_{ij} - 2 \text{sign}(y-x) \sqrt{f_i f_j} \int_x^y dx'' \phi_i(x'') \phi_j^*(x''). \quad (60)$$

Using LDA combined with bosonization, it is possible to deduce an approximate expression for the thermal one-body density matrix at large N :

$$\rho_{1B}(x, y) \simeq \frac{\mathcal{A} [n(x)n(y)]^{1/4}}{[\ell_T \sinh(\pi|x-y|/\ell_T)]^{1/2}}, \quad (61)$$

where \mathcal{A} is a constant, $n(x)$ is the thermal density profile given in Eq. (51), and $\ell_T = \hbar v_F / k_B T$ is the thermal length¹¹², with $v_F = \hbar \pi n(0) / m$ being the Fermi velocity at the center of the trap. It has been shown⁷⁸ that Eq. (61) gives results in very good agreement with those obtained by using the exact solution (58) already for $N = 10$.

E. Momentum distribution and Tan's contact

1. Momentum distribution at small and large k

The momentum distribution is one of the most common experimental observables, as it is measurable from time-of flight images of the atomic cloud after a sudden turn-off of the harmonic trap, assuming that interactions do not play any role during the expansion. This fact is ensured by the sudden drop of the density after switching off the confinement.

From the theoretical point of view, the momentum distribution is readily obtained as the Fourier transform of the one-body density matrix (see again Eq.(18)). The momentum distribution at small wavevector contains information about the off-diagonal long-range order: if there is a Bose-Einstein condensate, $n(k=0) = O(N)$ with N the total particle number. In the case of a TG gas in a harmonic trap, it was shown that³⁶ $n(k=0) \propto \sqrt{N}$. The effect of interactions and quantum fluctuations is so strong to destroy Bose-Einstein condensation, and we have only quasi off-diagonal long-range order. For arbitrary interactions, it is possible to generalize the previous result¹¹³ and one has $n(k=0) \propto N^\alpha$ with $\alpha \leq 1/2$. In the infinite size, homogeneous system the Luttinger liquid theory predicts the universal behaviour $n(k) \sim k^{1/2K-1}$ for any interaction strength, where $K(\gamma)$ is the Luttinger parameter¹¹⁴ which depends on interaction strength. This results holds for wavevectors smaller than the inverse of the interparticle distance, ie $k \leq n_0$ with n_0 the one-dimensional density. For finite systems of length L , the divergence is cut at small $k \sim 2\pi/L$.

At large wavevectors, another form of universality sets in and is related to contact interaction potential describing the ultracold gases. The one-body density matrix at short distance has a non-analytic behaviour at third order³⁶, i.e. $\rho_1(x, x') \sim |x-x'|^3$ implying a universal decay for wavevectors $k \geq n_0$ ^{67,115}

$$n(k) \sim k^{-4}. \quad (62)$$

This property originates from the cusp at short distance in the many-body wavefunction due to the contact (delta) interactions. It holds in all spatial dimensions and both at zero and at finite temperature.

2. Tan's contact

The Tan's contact \mathcal{C} is the weight of the large-momentum tails of the momentum distribution,

$$\mathcal{C} = \lim_{k \rightarrow \infty} n(k) k^4. \quad (63)$$

Tan's contact can be related to several many-body quantities, ranging from the interaction energy to the depletion rate by inelastic collisions, and many more¹¹⁶⁻¹¹⁹. Indeed it can be shown that

$$\mathcal{C} = \frac{gm^2}{\pi \hbar^4} \langle V_{int} \rangle = -\frac{m^2}{\pi \hbar^4} \frac{\partial E}{\partial g^{-1}}, \quad (64)$$

that in the $g \rightarrow \infty$ limit can be written

$$\mathcal{C} = \frac{m^2}{\pi \hbar^4} K. \quad (65)$$

We remind the reader that $K = -[\partial E / \partial g^{-1}]_{g \rightarrow \infty}$ and that we have shown that different values of K label the multiplet of strongly interacting mixtures (corresponding to the degenerate manifold in the limit $g \rightarrow \infty$) and that the ground-state corresponds to the largest value of K . This means that the different states with different symmetries can be labelled by the Tan's contact and that the ground-state corresponds to the largest value of \mathcal{C} , namely to the state with the largest momentum distribution tails.

3. Tan's contact for a trapped TG gas: exact results

In the TG limit, the contact does not depend on the interactions, K being the energy slope in the $g \rightarrow \infty$ limit [Eq. (65)]. This allows to write \mathcal{C} , in this regime, as a function of the corresponding non-interacting fermionic two-body density matrix $\rho_{2F}(x_1, x_2; x'_1, x'_2)$ ¹²⁰. Indeed for a TG gas, it can be shown that

$$\mathcal{C} = \frac{2}{\pi} \int_{-\infty}^{+\infty} F(x) dx \quad (66)$$

where we have defined

$$F(x) = \lim_{x', x'' \rightarrow x} \frac{\rho_{2F}(x', x; x'', x)}{|x - x'| |x - x''|}. \quad (67)$$

Eq. (66) holds at zero¹²⁰ and finite temperature, both in the canonical¹²¹ and grand-canonical ensembles¹⁰⁹. $F(x)$ can be written explicitly as a function of the single-particle orbitals $\phi_i(x)$,

$$F(x) = n(x) \sum_{i=1}^{\infty} |f_i \partial_x \phi_i(x)|^2 - \left| \sum_{i=1}^{\infty} f_i \phi_i(x) \partial_x \phi_i^*(x) \right|^2. \quad (68)$$

Eq. (68) is valid at zero temperature (where f_i becomes a step function) and at finite temperature in the grand-canonical ensemble¹⁰⁹. The explicit expression in the canonical ensemble has a similar but more complicated structure¹²¹.

Finally, remark that Eq. (66) is the (non-homogeneous) TG limit of the Lieb-Liniger contact expression

$$\mathcal{C}^{LL} = N(N-1)(m/\hbar^2)^2 g^2 \rho_2(0,0,0,0) \quad (69)$$

derived in [22]. Indeed since $\rho_2(0,0,0,0)$ scales as g^{-2} , the TG limit of Eq. (69) gives a finite value.

4. Tan's contact for trapped mixtures at finite interactions

Let ε be the ground-state energy density of a balanced homogeneous mixture and $\gamma = mg_{1D}/\hbar^2 \rho$ the dimensionless

interaction parameter, ρ being the total density. By using Eq. (64), one gets for the homogeneous gas

$$\mathcal{C} = g^2 \frac{m^2}{2\pi \hbar^4} L \rho^2 \frac{\partial e}{\partial \gamma} \quad (70)$$

where the dimensionless average ground-state energy per particle e is such that $\varepsilon(\rho) = \frac{\hbar^2}{2m} \rho^3 e(\gamma)$.

In the harmonically trapped system, it is possible to derive an expression for the contact by performing a LDA⁶⁷. We define the energy functional $E[\rho]$ of the density $\rho(x)$ which, in the LDA, reads

$$E[\rho] = \int dx [\varepsilon(\rho) + (V_{ext}(x) - \mu)\rho(x)]. \quad (71)$$

The ground-state density profile is obtained by minimizing the energy functional, i.e. setting $\partial E / \partial \rho = 0$. This yields an implicit equation for the density profile,

$$\frac{3}{2} \frac{\hbar^2}{m} \rho^2 e(\gamma) - \frac{g\rho}{2} \frac{\partial e}{\partial \gamma} = \mu - V_{ext}(x). \quad (72)$$

The chemical potential μ is fixed by imposing the normalization condition $N = \int dx \rho(x)$. Combining Eqs. (64), (71) and (72), we obtain Tan's contact within the LDA:

$$\mathcal{C}_{LDA} = g^2 \frac{m^2}{2\pi \hbar^4} \int dx \rho^2(x) \left. \frac{\partial e}{\partial \gamma} \right|_{\rho=\rho(x)}. \quad (73)$$

Generally $e(\gamma)$ is not known analytically. However, for the Lieb-Liniger gas it exists a very accurate analytical conjecture¹²² that allows to calculate the contact at any interactions. Moreover the asymptotic behaviour of $\lim_{\gamma \rightarrow \infty} e(\gamma)$ is known for the Lieb-Liniger gas as well as for balanced mixtures of $SU(\kappa)$ fermions. The case of an imbalanced Fermi gas (a trapped 1D Fermi system interacting with a single impurity) has been studied in [123]. In the strong-interacting limit, Eq. (73), takes the explicit form⁶⁷

$$\mathcal{C}_{LDA, g \rightarrow \infty}^{LL} = \frac{\sqrt{2} \times 128}{a_{ho}^3 45 \pi^3} N^{5/2}, \quad (74)$$

for Lieb-Liniger bosons and

$$\mathcal{C}_{LDA, g \rightarrow \infty}^{SU(\kappa), F} = \mathcal{C}_{LDA, g \rightarrow \infty}^{LL} Z_1(\kappa) \quad (75)$$

for $SU(\kappa)$ fermions⁸⁹, where $Z_1(\kappa) = -\frac{1}{\kappa} [\psi(\frac{1}{\kappa}) + C_{Euler}]$, ψ being the digamma function and C_{Euler} the Euler constant.

In the limit of infinitely strong repulsions it is possible to obtain an exact formula for the contact of a trapped mixture by using Eq. (65). For each spin component σ , it reads⁸²

$$\mathcal{C}_{\sigma}(\infty) = \frac{m^2}{2\pi \hbar^4} \sum_{\sigma'=1}^{\kappa} (1 + \delta_{\sigma\sigma'}) \sum_{P \in \mathcal{G}_N(k||\sigma, \sigma')} (a_p - a_{P(k, k+1)})^2 \alpha_k \quad (76)$$

where $\mathcal{G}_N(k||\sigma, \sigma')$ is the subset of permutations so that the indexes in positions k and $k+1$ correspond to particles belonging to components σ and σ' .

At finite temperature, the contact can be derived by the thermodynamic form of the Tan's relation (64)

$$\left(\frac{d\Omega}{da_{1D}}\right)_{\mu,T} = \frac{\pi\hbar^2}{m}\mathcal{C}, \quad (77)$$

where Ω is the grand thermodynamic potential. For the homogeneous Lieb-Liniger gas Ω can be calculated by solving two coupled equations, the Yang-Yang equations¹²⁴, while for bosonic or fermionic mixture one needs in principle to deal with an infinity of coupled equations that can be reduced to three complex coupled equations for the case of SU(2) fermions¹²⁵ or bosons¹²⁶. Once the grand thermodynamic potential is known as a function of the density, it is possible to calculate the contact for the thermal trapped system within the LDA scheme^{107,127}, the principle of the calculation being exactly the same as for the zero temperature gas. For the case of a thermal Lieb-Liniger gas and a SU(2) fermionic one, it has been shown that the contact can be written as

$$\mathcal{C}_{LDA} = \frac{N^{5/2}}{a_{ho}^3} f(\xi_\gamma, \xi_T), \quad (78)$$

where $f(\xi_\gamma, \xi_T)$ is a universal function depending only on the type of mixture and on the parameters $\xi_\gamma = a_{ho}/|a_{1D}|\sqrt{N}$ and $\xi_T = |a_{1D}|/\lambda_T$. One can also write Eq. (78) under the form $\mathcal{C}_{LDA} = N^{5/2}/a_{ho}^3 \zeta(\xi_\gamma, \tau)$ where ζ is a universal function of ξ_γ and $\tau = T/T_F$, or analogously as a function of two different combinations of ξ_γ and ξ_T . This writing allows to deduce the scaling properties of the contact in the thermodynamic limit at finite temperature. We will discuss this point deeply in Sec. II E 6.

5. Virial approach at large-temperature at strong interactions

Let us start from Eq. (77). Using a virial expansion for Ω , for a Lieb-Liniger gas one has

$$\mathcal{C}_{vir}^{LL} = \frac{4m\omega_0}{\hbar\lambda_T} N^2 c_2 \quad (79)$$

where $c_2 = \lambda_T \partial b_2 / \partial |a_{1D}|$, and $b_2 = \sum_{\nu} e^{-\beta E_{rel,\nu}}$, $\lambda_T = \sqrt{2\pi\hbar^2/(mk_B T)}$ being the De Broglie wavelength. For a harmonically-trapped gas $E_{rel,\nu} = \hbar\omega(\nu + 1/2)$, where ν 's are the solutions of the transcendental equation (8). In the TG regime, corresponding to $a_{1D} = 0$, one has $\nu = 2n + 1$, with $n \in \mathcal{N}$. In the strongly interacting regime $|a_{1D}|/a_{ho} \ll 1$, we get the following explicit expression for ν ¹²⁷

$$\sqrt{\frac{2}{2n+1}} \cot(\pi\nu/2) \simeq \sqrt{2} \frac{|a_{1D}|}{a_{ho}}. \quad (80)$$

This allows to obtain an analytical expression for c_2 as a function of ξ_T ,

$$c_2 = \sqrt{2} \left(\frac{1}{2\pi\xi_T^2} - \frac{e^{1/2\pi\xi_T^2}}{2^{3/2}\pi\xi_T^3} \text{Erfc}(1/\sqrt{2\pi}\xi_T) \right) \quad (81)$$

that is valid for *any* two interacting particles with the same mass: two bosons, two fermions or one boson and one fermion. Thus by inserting expression (81) in (79), one gets for the Lieb-Liniger gas

$$\mathcal{C}_{vir}^{LL} = \frac{2N^{5/2}}{\pi a_{ho}^3} \frac{\xi_\gamma}{\xi_T} \left(\sqrt{2} - \frac{e^{1/2\pi\xi_T^2}}{\xi_T} \text{Erfc}(1/\sqrt{2\pi}\xi_T) \right), \quad (82)$$

that in the TG limit simplifies to¹⁰⁹

$$\lim_{g \rightarrow \infty} \mathcal{C}_{vir}^{LL} = \frac{2\sqrt{2}}{a_{ho}^3} N^{5/2} \xi_\gamma \xi_T = \frac{N^{5/2}}{\pi^{3/2} a_{ho}^3} \sqrt{\tau}. \quad (83)$$

It is straightforward to show that^{89,107}, for the case of N SU(κ) balanced strongly interacting fermions $\mathcal{C}_{vir}^{SU(\kappa),F} = \mathcal{C}_{vir}^{LL}(\kappa - 1)/\kappa$.

6. Scaling properties

Eq. (78) gives the scaling laws for the contact at finite interaction and finite temperature in the thermodynamic limit ($N \gg 1$). This means that we can calculate $f(\xi_\gamma, \xi_T)$ for $N = 2$, for instance (if it easier to be calculated for $N = 2$) and even if the result once rescaled will not be applicable for small N , it will be valid for any $N \gg 1$. This because Eq. (78) has been derived by the Bethe Ansatz equations and on the LDA on the top of the them, and both are valid at large N . In order to cover the intermediate regime from few to many-body one can use instead the scaling function

$$\tilde{f}(\xi_\gamma, \tau) = \frac{\mathcal{C}_N(\xi_\gamma, \tau)}{\mathcal{C}_N(\infty, \tau)}. \quad (84)$$

Equation (84) holds in the regime of intermediate and large interaction ($\xi_\gamma \gtrsim 1$) in the following situations: (i) at $T = 0$ for a Lieb-Liniger gas and fermionic mixtures¹²⁸; (ii) for a Lieb-Liniger gas in the canonical ensemble at any temperature¹²¹; and for a Lieb-Liniger gas and SU(2) fermionic mixtures in the grand-canonical ensemble at large temperature^{107,121}. This means that in these regimes the contact for N particles in the $g \rightarrow \infty$ limit (the function $\mathcal{C}_N(\infty, \tau)$) contains all the N -dependency of the contact at almost any interactions.

III. RESULTS

A. Density profiles

As outlined in Sec. II B 1, the density profile for N TG bosons is the same as the density profile for N non-interacting fermions. In Fig. 5 we show the results obtained with the Green's function method for $N = 5, 10$ and 20 fermions compared with the corresponding Thomas-Fermi density profiles [Eq. (16)]. We observe a number of density oscillations equal to the number of particles, whose amplitude decreases with N . The position of these bumps correspond to the "classical" particles positions⁵⁰, namely to the position of the N delta

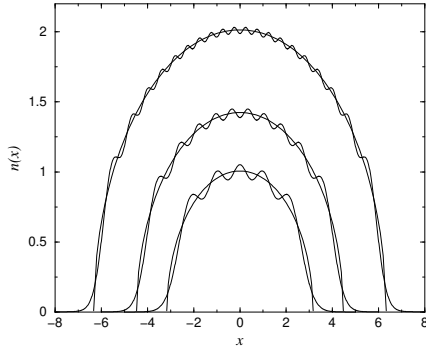


FIG. 5. From [129]. Exact particle density profile (bold lines) for $N = 5, 10$ and 20 harmonically confined fermions, compared with the corresponding profiles evaluated in the Thomas-Fermi approximation. Positions are in units of the characteristic length of the harmonic oscillator $a_{ho} = \sqrt{\hbar/(m\omega_0)}$ and the particle density in units of a_{ho}^{-1} . Reprinted figure with permission from [129], <https://doi.org/10.1103/PhysRevLett.85.2850>. Copyright (2021) by the American Physical Society.

peaks that one would get cutting the \hat{x} operator at the first N states, not considering highly unoccupied energy states. This shell effect persists for 2D and 3D fermions trapped in highly anisotropic harmonic trap⁵² at zero temperature. Temperature washes out this effect already at $k_B T \sim \hbar\omega_0$.

For the case of supersymmetric mixtures at infinitely strong interactions, the density profile can be calculated in an exact way by exploiting Eq. (32). Let x_i being the coordinate of a particle of the component of the mixture we are interested in, then the density for that component reads

$$n_\alpha(x) = \sum_{j=1}^N \rho_\alpha^{(j)} \rho_j(x) \quad (85)$$

with

$$\rho_j(x) = \int dx_1 \cdots \int dx_N \delta(x - x_i) \times \theta_P(x_1, \dots, x_N) |\Psi_A(x_1, \dots, x_N)|^2, \quad (86)$$

and $\rho_\alpha^{(j)} = \sum_{\{P\}} |a_P|^2$ being the α -spin density probability at position x_j ¹³⁰. In the above expression $\{P\}$ are the elements of the snippet basis where a particle of spin α is in position j . Remark that the a_P 's has the same symmetry of the trap. They are all equal in a box or in a ring trap, while in the harmonic potential they satisfy the property $a_i = a_{N-i+1}$. The resulting density profile depends on the state symmetry, but it can happen that states corresponding to different symmetries have the same density profiles. This is the case, for instance, of TG bosons and non-interacting fermions. In the first case the many-body wavefunction is fully symmetric while in the second case it is fully anti-symmetric.

In Figs. 6, 7 and 8 we show the density profiles for several harmonically trapped mixtures. Figure 6 shows the shape of the $\rho_j(x)$'s [Eq. (86)] for the case of 8 trapped particles, and

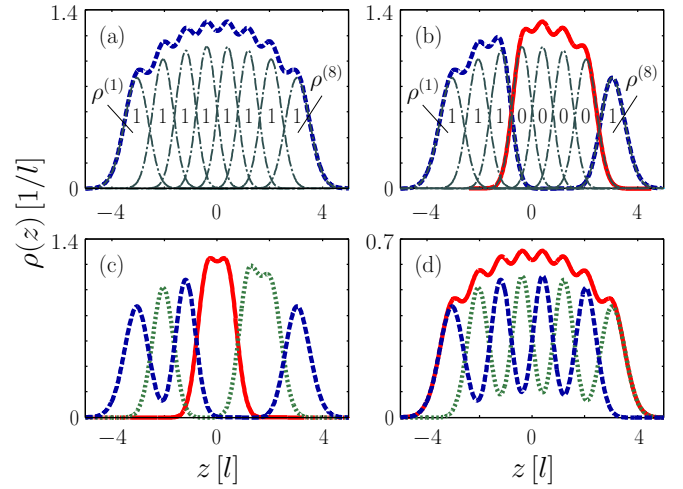


FIG. 6. From [85]. Spin densities of 8 spin-1 bosons in different symmetry configurations. Shown are the densities ρ_j (see Eq. (86)) (gray dash-dotted line), and the components n_0 (red solid line), n_1 (blue dashed line), and n_{-1} (green dotted line) of the spin density. Reprinted figure with permission from [85], <https://doi.org/10.1103/PhysRevLett.100.160405>. Copyright (2021) by the American Physical Society.

the spin-density profiles for a spin-1 boson gas, for different symmetry configurations.

Figure 7 focuses on balanced fermionic mixtures with $N = 6$ and $\kappa = 2, 3$ and 6 number of components. The symmetry of the many-body state is indicating by the corresponding Young tableau. The density for each component of the ground state (top panel of Fig. 7) is the same for any mixture up to a normalization factor. This is somehow due to the fact that their symmetry corresponds to a Young tableau (in the tree cases) that is a closed box. As soon as this sort of "Young tableau symmetry" is broken, the density profiles may change deeply for each component as shown for the case of excited states in the bottom panel of Fig. 7. The density profiles for boson-fermion mixtures have been studied in Refs.[132], [133] and [82]. Some examples are shown in Fig. 8. In the case of a boson-fermion mixture the ground state (the state corresponding to the largest slope energy) can never correspond to a "symmetric" Young tableau and the different components in the same mixture have different density profiles. For such a state (state 0, top panel), one observes a demixing behaviour with the bosonic components concentrates in the center of the trap and the fermionic ones more occupying the peripheral region of the trap.

B. Dynamical structure factor and spectral function

The TG solution allows also to access in an exact way to dynamical properties. In this section we focus on linear response regime, eg the response of the fluid to small perturbations. Large quenches and strongly out-of-equilibrium dynamics will be treated in Sec. III E below.

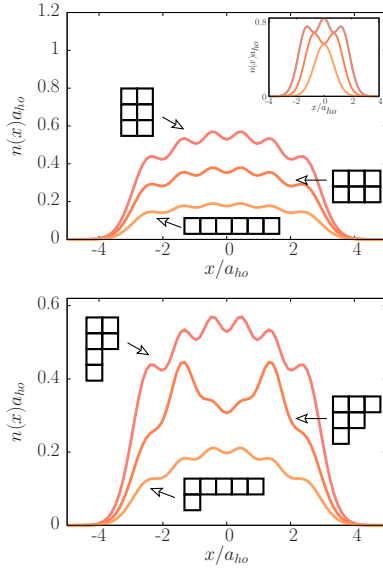


FIG. 7. From [131]. Density profiles for the ground state (top panel) and for the first many-body excited state with a symmetry different than the ground state (bottom panel) for three balanced mixtures (ie with the same number of particles in each species $N_1 = \dots = N_\kappa$) of strongly interacting Fermi gases, with different numbers of components $\kappa = 2, 3, 6$ and total particle number $N = 6$ (from top to bottom: $N_v = 3, 2, 1$). The density profiles are the same for each component of the mixture. The inset shows the corresponding ground state density profiles for the case of the corresponding mixtures of noninteracting fermions. Reprinted with permission from Decamp *et al.*, New J. Phys. **18**, 055011 (2016). Copyright 2016, (<https://doi.org/10.1088/1367-2630/18/5/055011>). Author(s) licensed under a Creative Commons Attribution 4.0 License.

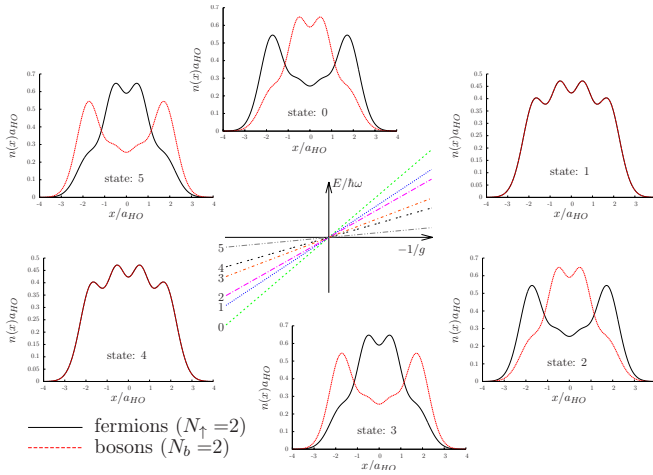


FIG. 8. From [134]. Density profiles for the six states with different symmetry for a mixture of 2 fermions and 2 bosons. Republished with permission of IOP Publishing, from *Analytical and numerical studies of Bose–Fermi mixtures in a one-dimensional harmonic trap*, A.S. Dehkarghani *et al.*, Journal of Physics B: Atomic, Molecular and Optical Physics **14**, 144002 (2017); permission conveyed through Copyright Clearance Center, Inc.

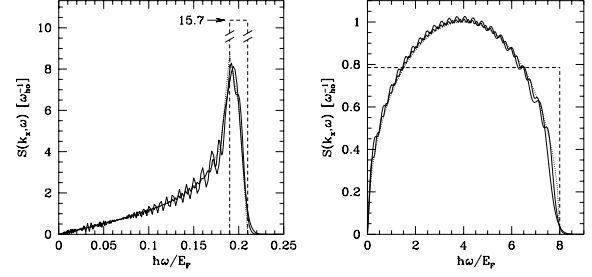


FIG. 9. From [79]. Dynamic structure factor of a TG gas under harmonic confinement. Left panel $k = 0.1k_F$, right panel $k = 2k_F$. The local density approximation (dots) is compared with the exact solution (lines) at various particle numbers. The dashed lines indicate the corresponding dynamic structure factor of a homogeneous gas. Reprinted figure with permission from [79], <https://doi.org/10.1103/PhysRevA.64.023421>. Copyright (2021) by the American Physical Society.

For a strongly correlated gas, both the spectral function and the dynamical structure factor are non-vanishing in a large part of the (k, ω) plane. Since the particles are interacting and fill an effective Fermi sphere, there are several ways for to adjust an excitation with transfer of a given momentum $\hbar k$ and energy $\hbar\omega$, noticeably by single or multiple particle-hole excitations. Due to the underlying Fermi sphere structure induced by correlations, in the homogeneous system there are also regions of the (k, ω) plane which are kinematically forbidden¹³⁵, for example, in the case of dynamical structure factor, at finite momentum $0 < k < 2k_F$ and small frequency, the first excitations possible are those who correspond to the backscattering processes $-k_F$ to k_F around the Fermi points.

In the homogeneous system, the non-linear Luttinger liquid approach^{135,136} provides a complete description of the spectral properties in proximity of each singularity line. Complementary to that approach, we provide here an exact analysis of the trapped case.

As a first illustration we present in Fig. 9 the results for the dynamical structure factor of a bosonic TG gas under harmonic confinement. Comparison with LDA shows that it provides a very good description of the spectrum if the energy transfer considered is much larger than the energy-level spacings ω_0 . The LDA approach has been used to predict the dynamical structure factors of bosons in a lattice plus harmonic trap confinement⁸⁰. The presence of the harmonic trap provides important qualitative changes in the shape of the dynamic structure factor as compared to the homogeneous case: in particular, due to the inhomogeneous density, the finite- k small- ω regions are in this case accessible to excitations.

The exact solution for the dynamical structure factor has been extended at finite temperature¹³⁷. As main effect of temperature, the backscattering region is washed out and higher energy excitations become possible.

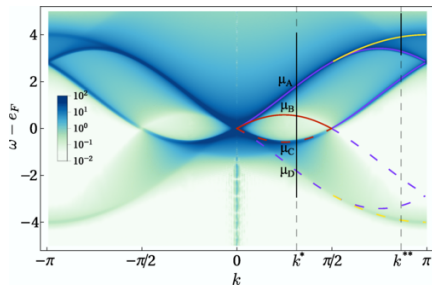


FIG. 10. From [47]. Spectral function of a TG gas on a lattice. The lines indicate the positions of the analogs of Lieb-I (red), Lieb-II (blue) branches and the third branch (yellow) typical of the lattice dispersion. Reprinted figure with permission from [47], <https://doi.org/10.1103/PhysRevLett.126.065301>. Copyright (2021) by the American Physical Society.

The dynamical structure factor can be also defined with respect to a non-equilibrium steady state: in this case its shape is considerably changed as compared to the ground-state one, reflecting the exotic nature of such state¹³⁸.

As a second example, we present the results for the spectral function of a Tonks-Girardeau gas on a lattice⁴⁷. Also in this case, the system is integrable only in the TG limit due to the presence of the external lattice potential and is shown in Fig. 10. The spectral function contains three main excitation singularities: two of them related to the corresponding branches in the homogeneous system, namely the Lieb-I and Lieb-II branches, and a third one appearing only in lattices and associated to the the existence of an inflection point in the single-particle dispersion. It is interesting to notice that the Lieb-II branch, which has vanishing spectral weight in the dynamical structure factor, has here a diverging singularity. The measurement of the spectral function could then allow to observe for the first time this eluding branch.

C. Momentum distribution

The momentum distribution of a harmonically trapped TG gas was obtained in Ref. [37]. An analytical closed formula for the momentum distribution of two TG bosons is also known¹³⁹. Since the momentum distribution is an off-diagonal observable, ie related to the one-body density matrix, its shape is different from the one of a spinless fermionic gas, which, in harmonic trap, coincides with the density profile. The momentum distribution of the TG gas displays a a unique central peak scaling with \sqrt{N} and algebraic tails at large momenta. Also, we notice that there are no oscillations. This is shown in Fig. 11. The authors of this work⁸⁵ have calculated the momentum distribution for 5 spin-1 bosons, for different wavefunction symmetries and have compared them to the one for 5 spinless fermions. The fully symmetric state corresponds to the spinless TG gas. For less symmetric states, the peak splits, and the momentum distribution develops oscillations, the more the state is anti-symmetric. The momentum distribution for particles with exchange symmetry depends on

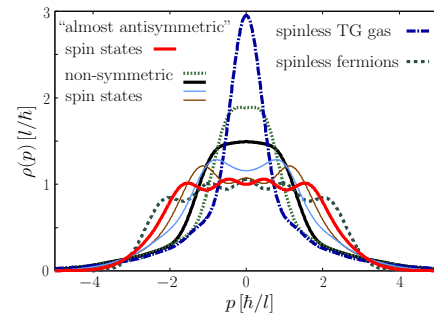


FIG. 11. From [85]. Momentum distribution of 5 spin-1 bosons in different symmetry configurations in comparison with the momentum distribution of 5 spinless fermions. Reprinted figure with permission from [85], <https://doi.org/10.1103/PhysRevLett.100.160405>. Copyright (2021) by the American Physical Society.

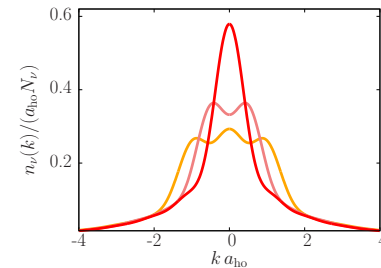


FIG. 12. From [89]. Momentum distribution for a balanced 6-component (red curve), 3-component (pink curve) and 2-component (orange curve) fermionic mixture with a total number of 6 fermions. Reprinted figure with permission from [89], <https://doi.org/10.1103/PhysRevA.94.053614>. Copyright (2021) by the American Physical Society.

the allowed symmetry and not really on the nature of the particles themselves¹⁴⁰. As an illustration of this idea, we show in Figs. 12 and 13 the momentum distribution for 6 particles. Fig. 12 corresponds to various choices of balanced fermionic mixtures whose density profiles are shown in Fig. 7. Fig. 13 refers to the ground-state for 3 spinless fermions and 3 identical bosons. The case of 6-component 6 fermions corresponds to a fully symmetric wavefunction and one finds a momentum distribution identical to that of a TG gas. For less symmetric cases, as for the spin-1 bosons, the momentum distribution develops a number of momentum density oscillations equal to the length of the longest column of the corresponding Young tableaux: 2 for the case of a 3-component 6-fermion mixture, 3 for the two-component case and for the 3-bosons-3-fermions mixture.

The effect of an impurity in a trapped Bose system with different mass ratio has been studied in [141].

At finite temperature, the momentum distribution of multi-component mixtures displays a crossover behaviour as a function of temperature T , going from a 'spin-ordered' state at low temperature to a 'spin-disordered' one at high temperature¹⁴².

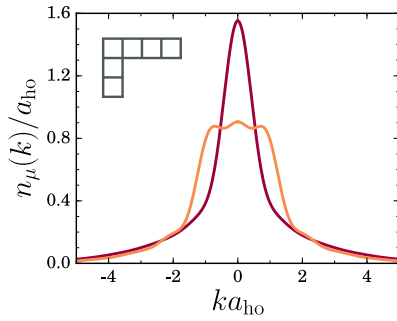


FIG. 13. From [82]. Momentum distribution for a mixture of 3 bosons and 3 fermions. The maroon line shows the bosonic momentum distribution and the orange line, the fermionic one. Reprinted with permission from Decamp *et al.*, New J. Phys. **19**, 125001 (2017). Copyright 2017, (<https://doi.org/10.1088/1367-2630/aa94ef>). Author(s) licensed under a Creative Commons Attribution 4.0 License.

The crossover occurs when $k_B T$ exceeds the energy difference among energy levels within the ground state manifold, hence the typical crossover temperature scales as $1/g$.

D. Tan's contact

As the momentum distribution depends on the wavefunction symmetry, the Tan's contact depends on it as well. In some way, the contact counts the many-body wavefunction cusps, thus more the wavefunction is symmetric, more the contact is sizeable. In the opposite situation, for a fully anti-symmetric state, the Tan's contact will be zero. In Fig. 14 we show the tails of the momentum distributions, drawn in Fig. 12, multiplied by k^4 : the asymptotic value at large k gives the Tan's contact. The largest contact corresponds to the fully-symmetric wavefunction (6 fermions, 6 components), the second to the two-rows diagram $\begin{array}{|c|c|} \hline \square & \square \\ \hline \square & \square \\ \hline \end{array}$ (6 fermions, 3 components) and the last to the diagram $\begin{array}{|c|} \hline \square \\ \hline \square \\ \hline \end{array}$ (6 fermions, 2 components). The Tan's contact is thus the fingerprint of the many-body wavefunction symmetry. Let us remark that the Tan's contact can be exactly calculated for two harmonically trapped bosons at any interaction strength¹²⁸,

$$\mathcal{C}_2(g) = \frac{m^2 g^2}{\pi \hbar^4} |\psi_V(0)|^2, \quad (87)$$

$\psi_V(x_{rel})$ being given in Eq. (9). Eq. (87) provides the well-known limit for the TG gas¹²¹: $\mathcal{C}_2(\infty) = (2/\pi)^{3/2} a_{ho}^{-3}$.

E. Dynamical properties and quenches

One strength point of the TG solution is the possibility to describe the arbitrary quantum dynamics, including situations strongly out-of-equilibrium.

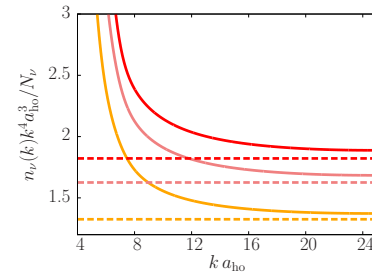


FIG. 14. From [89]. Tan's contact $(n(k)k^4)$ for a balanced 6-component (red curve), 3-component (pink curve) and 2-component (orange curve) fermionic mixture with a total number of 6 fermions. The data are the same of those of Fig. 12. The asymptotic values (horizontal lines) have been evaluated from Eq. (76). Reprinted figure with permission from [89], <https://doi.org/10.1103/PhysRevA.94.053614>. Copyright (2021) by the American Physical Society.

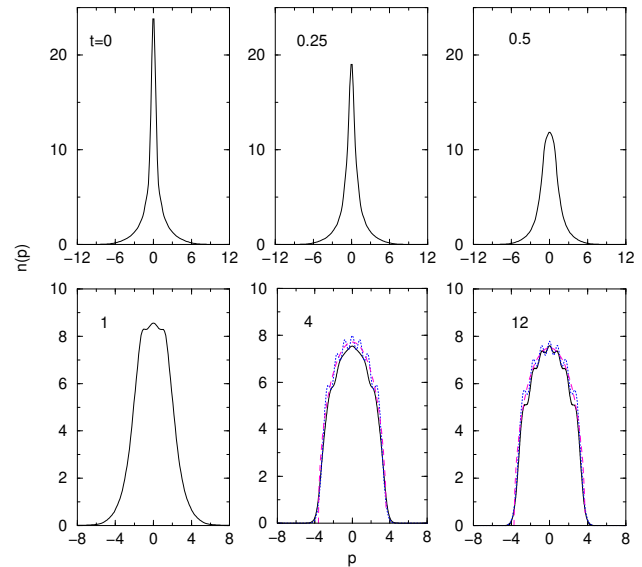


FIG. 15. From [41]. Momentum distribution (in units of \hbar/a_{ho}) as a function of time (in units of ω_0^{-1}) of an expanding TG gas following a sudden turn-off of the harmonic potential. At long times, the momentum distribution tends to the one of an equilibrium Fermi gas under harmonic confinement. Reprinted figure with permission from [41], <https://doi.org/10.1103/PhysRevLett.94.240404>. Copyright (2021) by the American Physical Society.

As first example, we describe the dynamics of a TG gas following a sudden turn-off of the harmonic confinement $V_{ext}(x,t) = m\omega^2(t)x^2/2$ with $\omega(t) = \omega_0$ for $t < 0$ and $\omega(t) = 0$ for $t \geq 0$. Notice that there is no expansion in the transverse direction, the motion corresponds to the expansion inside a one-dimensional waveguide. For this reason, at difference from the usual three-dimensional expansion, interactions during expansion cannot be neglected and indeed strongly influence the dynamics.

To describe the dynamics we use the time-dependent Bose-

Fermi mapping (see Sec. II A). The specific expansion dynamics can be solved exactly at arbitrary times⁴¹ by introducing a scaling parameter $b(t) = \sqrt{1 + \omega_0^2 t^2}$ associated to the size of the density profile during the expansion and a dynamical phase. The TG wavefunction is then expressed in terms of the one at initial times according to

$$\Phi_B(x_1, \dots, x_N; t) = b^{-N/2} \Phi_B(x_1/b, \dots, x_N/b; 0) \times \exp\left(\frac{ib}{b\omega_0} \sum_j \frac{x_j^2}{2a_{ho}^2}\right) \exp\left(-i \sum_j \varepsilon_j \tau\right). \quad (88)$$

This solution allows to calculate several properties, such as the time-dependent density profile and the momentum distribution. A remarkable prediction stemming from the above solution is that the momentum distribution at long times tends to the one of a non-interacting Fermi gas ("dynamical fermionization") as also observed in numerical simulations on a lattice¹⁴³ and experimentally¹³. The state of the system at such long times is well described by generalized Gibbs Ensemble and the equilibration mechanism has been elucidated in terms of interference effects^{144,145}.

The same type of solution describes also a partial opening of the trap, described by $\omega(t \leq 0) = \omega_0$ and $\omega(t) = \omega_1$ for $t > 0$. This excites a large-amplitude breathing mode. Correspondingly, the momentum distribution oscillates in time between the one of a TG gas and a fermionic one⁴¹. A remarkable feature of the oscillation is that it is undamped. This is related to integrability and constrained dynamics in one dimension. At finite temperature the exact TG solution predicts a many-body bounce effect¹⁴⁶, ie the narrowing of the momentum distribution at twice the rate of oscillations of the density profile. Frequency doubling in momentum space was also experimentally observed at weak interactions¹⁴⁷. At strong finite interactions, no exact theory is available but Generalized Hydrodynamics^{148,149} well accounts for the quench dynamics observed in the experiment¹⁴.

The role of confining potential in the quench dynamics has also been explored. The release of a TG gas from a hard wall trap was studied, and a notable difference was found on the scaling of the thermalization time with particle number¹⁵⁰. The dynamics of a TG gas following a sudden change of trap strength for a quartic potential was addressed in Ref.[151], showing that interparticle collisions allow the TG gas to decohere more quickly than a non-interacting Fermi gas, due to different properties of the off-diagonal part of the one-body density matrix of the two gases. The same work also pointed out the different dynamical behaviour of TG bosons and ideal fermions in shortcut-to-adiabaticity protocols.

The exact solution for the arbitrary quantum dynamics can be used to access to a wealth of dynamical problems and regimes. For example, it is possible to follow the dynamics of a TG gas in presence of a barrier potential. Ref.[152] reports of the equivalent of the optical Talbot effect in the dynamics following the sudden turn off of an eccentric barrier potential. Barrier renormalization effects due to quantum fluctuations can be probed by the time evolution following sudden displacement of a harmonic trap split by a barrier¹⁰³. The dynamics of population imbalance across a barrier allows to

follow the Josephson oscillations among tunnel-coupled one-dimensional tubes in a head-to-tail configuration. The exact TG solution has provided a stringent test of the Luttinger-liquid theory predictions and highlighted some low-energy excitation modes responsible for the damping of the Josephson oscillations¹⁰⁴.

Putting a TG gas on a ring, one can follow the current flows. Also in this case, important information can be obtained from the exact TG solution. For example, it has been shown that in presence of a weak barrier potential, an initially phase imprinted current undergoes coherent oscillations, ie it displays quantum coherent phase slips. The TG solution allows to access to the nature of the state during the dynamics and show that multi particle-hole oscillations play a major role¹⁰⁵.

Large-amplitude quench dynamics can also be engineered to give rise to dispersive shock waves in TG gases. Two protocols have been proposed: i) a sudden change of a localised external potential^{153,154} and ii) a quantum fluid hitting against the hard walls of its container¹⁰⁶.

A phenomenological model for the dynamics of an output-coupled TG gas traversing its parent cloud as the one experimentally realized in Ref. [26] was proposed in Ref. [155].

Other types of quenches allow to study phase transitions, as eg it is the case for the pinning and commensurate-incommensurate transition in the presence of an optical lattice. A sudden turn off of the optical lattice gives rise to a dynamical depinning of the TG gas¹⁵⁶ and the sudden set into motion of the lattice allows to probe the various phases¹⁵⁷.

The quench dynamics of fermionic gases with strong repulsions has also attracted some attention. The dynamics of SU(κ) fermions following a sudden change of the trapping potential was addressed in Ref. [93], finding a decoupling of density and spin dynamics and suppression of the latter. Ref. [98] proposes a setup to observe the spin mixing dynamics following an initially fully imbalanced state, and finds universal oscillations and superdiffusion magnetization dynamics. This last result, already predicted¹⁵⁸ and observed¹⁵⁹ for a 1D homogeneous spin system, shows that superdiffusion persists also in the presence of an external potential that breaks the integrability of the system.

F. Finite temperature results

Signatures of quantum correlation, as the shell effects in the density profiles, and in the bulk of the momentum distribution are washed out already at temperatures of the order of the harmonic oscillator energy spacing $T \sim \hbar\omega_0/k_B$. This is shown in Fig. 16 for the density profiles of $N = 4$ and 20 TG bosons¹⁶⁰ and in the first panel of Fig. 17 for the momentum distribution of 5 TG bosons at increasing temperatures.

However, the contact in 1D is surprisingly robust against temperature. It is even better: in the TG regime it increases with the temperature¹⁰⁹, as we have shown in Eq. (83). This counter-intuitive result is shown in the inset of top panel of Fig. 17 and in the bottom panel of the same figure. The temperature does not wash out the cusps in the hard-core limit and moreover allows the particles to get closer, increasing the

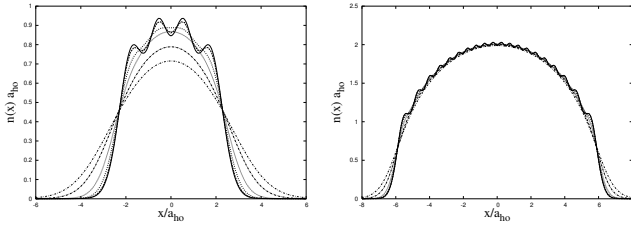


FIG. 16. From [160]. Particle density profile for $N = 4$ (left panel) and $N = 20$ (right panel) harmonically confined TG bosons (or non-interacting fermions) at various values of the temperature. $T = 0$ (solid curve) and $T = 0.2\hbar\omega_0/k_B$ (dashed curve); the other curves refer to $k_B T/\hbar\omega_0 = 0.5, 1.0, 2.0$ and 3.0 , in order of decreasing peak height. Reprinted figure with permission from [160], <https://doi.org/10.1103/PhysRevA.66.055601>. Copyright (2021) by the American Physical Society.

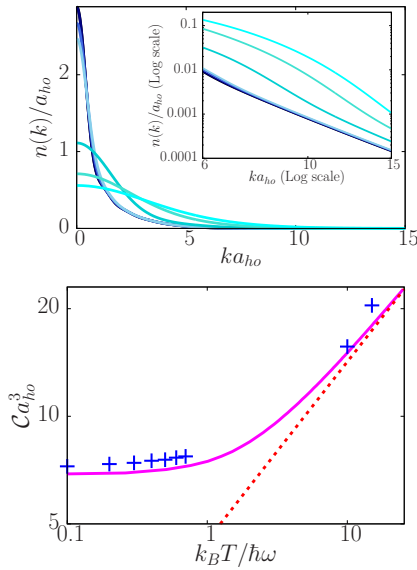


FIG. 17. From [109]. Top panel: momentum distribution of a TG gas (in units of a_{ho}) as a function of wavevector (in units of $1/a_{ho}$) with $N = 5$ particles under harmonic confinement at increasing temperature, from top to bottom in the main peak $k_B T/\hbar\omega_0 = 0.1, 0.5, 0.7, 5, 10, 15$. Bottom panel: Tan's contact (in units of a_{ho}^3) as a function of temperature $k_B T$ (in units of $\hbar\omega_0$) for a TG gas under harmonic confinement. The expression from (66) and (solid, magenta) is compared with the high-temperature limit (83) (dashed, red) and the data from the numerical calculation of the momentum distribution (crosses, blue). Reprinted figure with permission from [109], <https://doi.org/10.1103/PhysRevLett.110.020403>. Copyright (2021) by the American Physical Society.

slope of the wavefunction in the neighbourhood of the cusps, thus increasing the contact.

At finite interaction, in the harmonically trapped system, the contact first increases with the temperature till the value $T_{max} \simeq mg^2/(8\hbar^2 k_B)$ and then decreases¹²⁷. This can be deduced from the virial expression (82). The maximum marks the crossover between the fermionized regime and the ideal

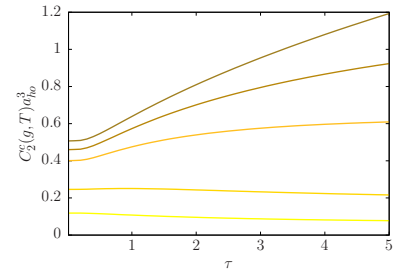


FIG. 18. From [121]. Canonical Tan's contact $\mathcal{C}_2^c(g, T)$ as a function of $\tau = T/T_F$ for different values of the interaction strength $z = a_{ho}/(|a_{1D}|\sqrt{N})$. From bottom to top: $z = 0.5, 1, 2.5, 5$, and 1000 . The curve for $z = 1000$ is indiscernible from the contact evaluated in the TG limit (89). Reprinted figure with permission from [121], <https://doi.org/10.1103/PhysRevA.100.063608>. Copyright (2021) by the American Physical Society.

boson gas. In the TG regime the position of this maximum tends to infinity (83) since fermionization persists at any temperature.

At finite interactions and finite temperature, the contact for a harmonically trapped system can be exactly calculated only for two particles, since the whole spectrum is known⁴³. An analytical expression can be derived for the case of two TG bosons (in the canonical ensemble). It reads

$$\mathcal{C}_2^c(\infty, T) = \frac{\sqrt{32}}{\pi^{3/2} a_{ho}^3} Z_r^{-1} \sum_j e^{-\beta\hbar\omega_0(2j-1)} \frac{(2j-1)!!}{2^j(j-1)!}, \quad (89)$$

with $Z_r = \sum_j e^{-\beta\hbar\omega_0(2j-1)}$. One can readily check that the zero-temperature limit of Eq. (89) yields $\mathcal{C}_2(\infty, 0) = (2/\pi)^{3/2} a_{ho}^3$. The results for the contact of two bosons as a function of the temperature for various values of interaction strength are shown in Fig. 18. We will see in the next section that the two-body calculation encloses an essential part of the contact for N particles.

G. Scaling properties

In the regimes discussed in Sec. II E 6, where Eq. (84) holds for any N , we can write

$$\mathcal{C}_N(\xi_\gamma, \tau) = \mathcal{C}_2(\xi_\gamma, \tau) \frac{\mathcal{C}_N(\infty, \tau)}{\mathcal{C}_2(\infty, \tau)}. \quad (90)$$

Eq. (90) can be interpreted as follows: (i) at each temperature the way in which particles see each other at a given interaction strength is given by the two-body calculation; (ii) the correlation contribution due to the fact that the particles are N and not only two, is embedded in the contact at in the $g \rightarrow \infty$ limit calculated at the same temperature. Let us underline that both the two-body contact at finite temperature and interaction strength, and the contact for N TG particles at finite temperature can be calculated exactly. Moreover, for the canonical

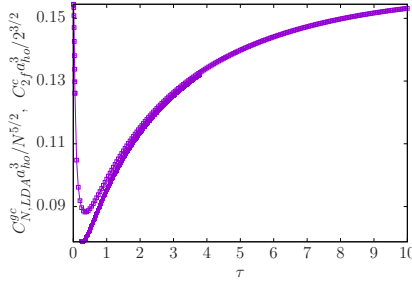


FIG. 19. From [107]. LDA grand canonical contact $\mathcal{C}_{N,LDA}^{gc}$ rescaled by $N^{5/2}$ (full symbols) and the canonical one \mathcal{C}_{2f}^c for two fermions (empty symbols) rescaled by $N^{3/2}(N-1) = 2^{3/2}$ as functions of $\tau = T/T_F$, for the case $\xi_\gamma = 3.53$. Reprinted figure with permission from [107], <https://doi.org/10.1103/PhysRevA.101.013633>. Copyright (2021) by the American Physical Society.

ensemble, that is the relevant case for experiments, it exists an analytical Ansatz for the finite-temperature TG gas contact¹²¹

$$\begin{aligned} \mathcal{C}_N^c(\infty, \tau) &= h_2(\infty, \tau) s(N) \\ &= h_2(\infty, \tau) \left(N^{5/2} - N^{3/4(1+\exp(-2/\tau))} \right), \end{aligned} \quad (91)$$

where

$$h_2(\infty, \tau) = \mathcal{C}_2(\infty, T(\tau)) / s(2). \quad (92)$$

The function $s(N)$ interpolates between the $(N^{5/2} - N^{3/4})$ scaling at zero temperature¹²⁸ and the $(N^{5/2} - N^{3/2})$ scaling for canonical ensembles at large temperature¹²¹. We expect Eq. (90) to hold also for boson-boson and boson-fermion mixtures at zero temperature and at very large temperatures, both in the canonical and grand-canonical ensembles.

More challenging is the analysis of multi-component mixtures at finite, low temperatures^{107,125,142}. In this regime there is a sort of symmetry mixing with differing weights depending on the temperature and the symmetry itself, that causes a rapidly drop of the contact with the temperature. The characteristic temperature T_0 of such a symmetry blending, for the trapped system and in the strong interacting limit, scales with the ground-state contact in the $g \rightarrow \infty$ limit divided by the interaction strength¹⁰⁷. Thus, in such limit, the drop of the contact is a discontinuous jump at $T = 0$ ($T_0 \rightarrow 0$). This means that, in this range of temperature, $\mathcal{C}_N(\infty, T)$ cannot catch the N dependence of $\mathcal{C}_N(g, T)$ at finite g , that is a continuous function of the temperature. However, for the case of a SU(2) fermionic mixture, by performing a LDA calculation on the top of the thermodynamics Bethe Ansatz equations¹²⁵ and a two-body calculation, it has been shown¹⁰⁷ that it is possible to obtain a lower bound and an upper bound for the rescaled grand-canonical contact $\mathcal{C}_N(g, T)^{gc} / N^{5/2}$ or for the canonical one $\mathcal{C}_N(g, T)^c / (N^{5/2} - N^{3/2})$. These two curves are shown in Fig. 19.

IV. CONCLUSIONS AND OUTLOOK

In this review we have illustrated the various techniques to obtain and exploit the exact solutions for strongly-interacting one-dimensional trapped bosons, fermions and mixtures. Infinite interactions play the same role as the Pauli principle, allowing the mapping of the many-body wavefunction for the strongly correlated many-body system onto that for a system of spinless non-interacting fermions. The knowledge of the exact wavefunction gives a unique opportunity to unveil the properties of strongly correlated one-dimensional fluids. It also allows to understand of the role of particle-exchange symmetries in the mixtures. Moreover, it allows to benchmark both classical numerical simulators, usually used for systems at finite interaction and temperature, as well as particular experimental setups for quantum simulators. One example is provided by the mapping of strongly interacting fermions onto a spin chain^{18,84,161,162}. The exact solution allows also to provide tests of other approximate approaches, as the Luttinger liquid solution, as done eg in Refs. [163], and [104].

The detailed study of the predictions of the Girardeau mapping has yielded a wealth of information on the properties of the 1D fluids: for example, the study of the dynamical structure factor shows the effects of the curvature of the dispersion of the collective excitation modes and its broadening due to particle-hole excitations; both effects are not included in the usual Luttinger liquid picture, but require non-linear Luttinger liquid tools¹⁶⁴. Another striking prediction of the TG solution is the fact that large-amplitude breathing modes in a harmonic trap are not damped. This has stimulated very general reflections on damping and thermalization in closed quantum systems, and about the fate of the system at very long times¹⁶⁵, which were then followed by the experiment on the quantum Newton's cradle²⁵. In multicomponent Fermi gases, it has been demonstrated that the tails of the momentum distribution are fixed by the symmetry of the mixture⁸⁹ thus providing a new type of symmetry spectroscopy. Furthermore, the dynamics of the magnetization of strongly repulsive SU(2) fermions in harmonic trap⁹⁸ points to a connection to the Kardar-Parisi-Zhang universality class^{158,166}, a statistical physics model describing the growth and roughening of classical interfaces¹⁶⁷.

Several directions open up in this research field. First of all, even if we have shown that these techniques can be applied not only for the case of zero-temperature systems at the equilibrium, but also for the case of finite temperature and for the full quantum dynamics, there is a real challenge to find new strategies in order to be able to deal with the amazing increasing complexity arising when more and more single-particle orbitals have to be included in the calculations. In particular, there is a clear need to improve the existing solution strategies in order to reach eg larger system sizes, or describe arbitrary temperatures. In this respect, it is very useful to share open source codes as done eg in [168] and [130]. Secondly, the solutions illustrated in this review could be used to explore further the physical properties of correlated gases. This is extremely useful since these solutions are amongst the very rare cases where one can follow exactly the arbitrary dynam-

ics even at long times. This will allow to describe specific dynamical protocols useful for quantum information and quantum state engineering, or predict the outcome of novel quench protocols. For example, a quantum heat engine was recently designed exploiting the TG solution¹⁵¹, and quantum simulation of the spin-Seebeck effect was proposed by exploiting the mapping to the inhomogeneous Heisenberg chain¹⁶⁹. Finally, the quest is still open to find other exact solutions, as eg for the case of particles of unequal masses^{170–173}.

DATA AVAILABILITY

The data that support the findings presented in this review are available from the corresponding authors of the original publications upon reasonable request.

ACKNOWLEDGMENTS

We are grateful to M. Albert, T. Busch, D.M. Gangardt, J. Polo Gomez, M. Olshanii, G. Pecci, L. Santos and N.T. Zinner for their comments and suggestions on the manuscript. We acknowledge funding from the ANR-21-CE47-0009 Quantum-SOPHA project.

AUTHOR DECLARATIONS

Conflict of interest

The authors have no conflicts to disclose.

- ¹E. H. Lieb, “Exact analysis of an interacting Bose gas. II. the excitation spectrum,” *Phys. Rev.* **130**, 1616 (1963).
- ²C. N. Yang, “Some exact results for the many-body problem in one dimension with repulsive delta-function interaction,” *Phys. Rev. Lett.* **19**, 1312–1315 (1967).
- ³B. Sutherland, “Further results for the many-body problem in one dimension,” *Phys. Rev. Lett.* **20**, 98–100 (1968).
- ⁴M. D. Girardeau, “Relationship between systems of impenetrable bosons and fermions in one dimension,” *J. Math. Phys.* **1**, 516 (1960).
- ⁵V. Yurovsky, M. Olshanii, and D. Weiss, “Collisions, correlations, and integrability in atom waveguides,” *Advances in atomic, molecular and optical physics* **55**, 61 (2008).
- ⁶M. A. Cazalilla, R. Citro, T. Giamarchi, E. Orignac, and M. Rigol, “One dimensional bosons: From condensed matter systems to ultracold gases,” *Rev. Mod. Phys.* **83**, 1405–1466 (2011).
- ⁷X.-W. Guan, M. T. Batchelor, and C. Lee, “Fermi gases in one dimension: From Bethe ansatz to experiments,” *Rev. Mod. Phys.* **85**, 1633–1691 (2013).
- ⁸T. Sowiński and M. Á. García-March, “One-dimensional mixtures of several ultracold atoms: a review,” *Reports on Progress in Physics* **82**, 104401 (2019).
- ⁹T. Kinoshita, T. R. Wenger, and D. S. Weiss, “Observation of a one-dimensional Tonks-Girardeau gas,” *Science* **305**, 5687 (2004).
- ¹⁰B. Paredes, A. Widera, V. Murg, O. Mandel, S. Fölling, I. Cirac, G. Shlyapnikov, T. Hansch, and I. Bloch, “Tonks-Girardeau gas of ultracold atoms in an optical lattice,” *Nature* **429**, 277 (2004).
- ¹¹H. Moritz, T. Stöferle, K. Günter, M. Köhl, and T. Esslinger, “Confinement induced molecules in a 1d Fermi gas,” *Phys. Rev. Lett.* **94**, 210401 (2005).

- ¹²T. Kinoshita, T. Wenger, and D. S. Weiss, “Local pair correlations in one-dimensional Bose gases,” *Phys. Rev. Lett.* **95**, 190406 (2005).
- ¹³J. Wilson, N. Malvania, Y. Le, Y. Zhang, M. Rigol, and D. Weiss, “Observation of dynamical fermionization,” *Science* **367**, 1461 (2020).
- ¹⁴N. Malvania, Y. Zhang, Y. Le, J. Dubail, M. Rigol, and D. S. Weiss, “Generalized hydrodynamics in strongly interacting 1d Bose gases,” *Science* **373**, 1129–1133 (2021), <https://www.science.org/doi/pdf/10.1126/science.abf0147>.
- ¹⁵G. Zürn, F. Serwane, T. Lompe, A. N. Wenz, M. G. Ries, J. E. Bohn, and S. Jochim, “Fermionization of two distinguishable fermions,” *Phys. Rev. Lett.* **108**, 075303 (2012).
- ¹⁶G. Pagano, M. Mancini, P. Lombardi, G. Cappellini, P. Lombardi, K.-J. L. F. Schafer, H. Hu, J. Catani, C. Sias, M. Inguscio, and L. Fallani, “A one-dimensional liquid of fermions with tunable spin,” *Nature Physics* **10**, 198–201 (2014).
- ¹⁷Y. an Liao, A. S. C. Rittner, T. Paprotta, W. Li, R. G. H. Guthrie B. Partridge, S. K. Baur, and E. J. Mueller, “Spin-imbalance in a one-dimensional Fermi gas,” *Nature* **467**, 567 (2010).
- ¹⁸S. Murmann, F. Deuretzbacher, G. Zürn, J. Bjerlin, S. M. Reimann, L. Santos, T. Lompe, and S. Jochim, “Antiferromagnetic Heisenberg spin chain of a few cold atoms in a one-dimensional trap,” *Phys. Rev. Lett.* **115**, 215301 (2015).
- ¹⁹G. Zürn, A. N. Wenz, S. Murmann, A. Bergschneider, T. Lompe, and S. Jochim, “Pairing in few-fermion systems with attractive interactions,” *Phys. Rev. Lett.* **111**, 175302 (2013).
- ²⁰T. Jacqmin, J. Armijo, T. Berrada, K. V. Kheruntsyan, and I. Bouchoule, “Sub-poissonian fluctuations in a 1d Bose gas: From the quantum quasicondensate to the strongly interacting regime,” *Phys. Rev. Lett.* **106**, 230405 (2011).
- ²¹E. Haller, M. Goustavsson, M. Mark, J. Danzl, R. Hart, G. Pupillo, and H.-C. Nägerl, “Realization of an excited, strongly correlated quantum gas phase,” *Science* **325**, 1224 (2009).
- ²²D. M. Gangardt and G. V. Shlyapnikov, “Stability and phase coherence of trapped 1d Bose gases,” *Phys. Rev. Lett.* **90**, 010401 (2003).
- ²³N. Fabbri, M. Panfil, D. Clément, L. Fallani, M. Inguscio, C. Fort, and J.-S. Caux, “Dynamical structure factor of one-dimensional Bose gases: Experimental signatures of beyond-luttinger-liquid physics,” *Phys. Rev. A* **91**, 043617 (2015).
- ²⁴S. Hofferberth, I. Lesanovsky, B. Fischer, T. Schumm, and J. Schmiedmayer, “Non-equilibrium coherence dynamics in one-dimensional Bose gases,” *Nature* **449**, 324 (2007).
- ²⁵T. Kinoshita, T. R. Wenger, and D. S. Weiss, “A quantum Newton’s cradle,” *Nature* **440**, 900 (2006).
- ²⁶S. Palzer, C. Zipkes, C. Sias, and M. Köhl, “Quantum transport through a Tonks-Girardeau gas,” *Phys. Rev. Lett.* **103**, 150601 (2009).
- ²⁷J. Catani, G. Lamporesi, D. Naik, M. Gring, M. Inguscio, F. Minardi, A. Kantian, and T. Giamarchi, “Quantum dynamics of impurities in a one-dimensional Bose gas,” *Phys. Rev. A* **85**, 023623 (2012).
- ²⁸F. Meinert, M. Knap, E. Kirilov, K. Jag-Lauber, M. Zvonarev, E. Demler, and H.-C. Nägerl, “Bloch oscillations in the absence of a lattice,” *Science* **356**, 945 (2017).
- ²⁹M. Olshanii, “Atomic scattering in the presence of an external confinement and a gas of impenetrable bosons,” *Phys. Rev. Lett.* **81**, 938 (1998).
- ³⁰E. Lieb, *Phys. Rev.* **130**, 1616 (1963).
- ³¹P. Jordan and E. Wigner, “Über das paulische Äquivalenzverbot,” *Zeitschrift für Physik* **47**, 631 (1928).
- ³²M. D. Girardeau, “Anyon-fermion mapping and applications to ultracold gases in tight waveguides,” *Phys. Rev. Lett.* **97**, 100402 (2006).
- ³³R. Santachiara and P. Calabrese, “One-particle density matrix and momentum distribution function of one-dimensional anyon gases,” *Journal of Statistical Mechanics: Theory and Experiment* **2008**, P06005 (2008).
- ³⁴M. Burrello and A. Trombettoni, “Non-abelian anyons from degenerate landau levels of ultracold atoms in artificial gauge potentials,” *Phys. Rev. Lett.* **105**, 125304 (2010).
- ³⁵O. I. Pâtu, “Nonequilibrium dynamics of the anyonic Tonks-Girardeau gas at finite temperature,” *Phys. Rev. A* **102**, 043303 (2020).
- ³⁶P. J. Forrester, N. E. Frankel, T. M. Garoni, and N. S. Witte, “Finite one-dimensional impenetrable Bose systems: Occupation numbers,” *Phys. Rev. A* **67**, 043607 (2003).

- ³⁷M. Girardeau, E. Wright, and J. Triscari, “Ground-state properties of a one-dimensional system of hard-core bosons in a harmonic trap,” *Phys. Rev. A* **63**, 033601 (2001).
- ³⁸T. Papenbrock, “Ground-state properties of hard-core bosons in one-dimensional harmonic traps,” *Phys. Rev. A* **67**, 041601 (2003).
- ³⁹D. S. Dean, P. Le Doussal, S. N. Majumdar, and G. Schehr, “Noninteracting fermions in a trap and random matrix theory,” *J. Phys. A: Math. Theor.* **52**, 144006 (2019).
- ⁴⁰M. D. Girardeau and E. M. Wright, “—,” *Phys. Rev. Lett.* **84**, 5691 (2000).
- ⁴¹A. Minguzzi and D. Gangardt, “Exact coherent states of a harmonically confined Tonks-Girardeau gas,” *Phys. Rev. Lett.* **94**, 240404 (2005).
- ⁴²A. Colcelli, G. Mussardo, G. Sierra, and A. Trombettoni, “Integrable floquet hamiltonian for a periodically tilted 1d gas,” *Phys. Rev. Lett.* **123**, 130401 (2019).
- ⁴³T. Busch, B.-G. Englert, K. Rzazewski, and M. Wilkens, “Two cold atoms in a harmonic trap,” *Found. Phys.* **28**, 549 (1998).
- ⁴⁴M. Rigol and A. Muramatsu, “Ground-state properties of hard-core bosons confined on one-dimensional optical lattices,” *Phys. Rev. A* **72**, 013604 (2005).
- ⁴⁵B. Paredes, A. Widera, V. Murg, O. Mandel, S. Fölling, I. Cirac, G. V. Shlyapnikov, T. W. Hänsch, and I. Bloch, “Tonks-Girardeau gas of ultracold atoms in an optical lattice,” *Nature* **429**, 277 (2004).
- ⁴⁶M. Rigol, “Finite-temperature properties of hard-core bosons confined on one-dimensional optical lattices,” *Phys. Rev. A* **72**, 063607 (2005).
- ⁴⁷J. Settino, N. Lo Gullo, F. Plastina, and A. Minguzzi, “Exact spectral function of a Tonks-Girardeau gas in a lattice,” *Phys. Rev. Lett.* **126**, 065301 (2021).
- ⁴⁸P. Vignolo, A. Minguzzi, and M. P. Tosi, “Exact particle and kinetic-energy densities for one-dimensional confined gases of noninteracting fermions,” *Phys. Rev. Lett.* **85**, 2850–2853 (2000).
- ⁴⁹P. D. Kirkman and J. B. Pendry, “The statistics of one-dimensional resistances,” *Journal of Physics C: Solid State Physics* **17**, 4327 (1984).
- ⁵⁰P. Vignolo, A. Minguzzi, and M. P. Tosi, “Degenerate gases under harmonic confinement in one dimension: rigorous results in the impenetrable-bosons/spin-polarized-fermions limit,” *International Journal of Modern Physics B* **16**, 2161–2184 (2002).
- ⁵¹N. H. March and L. M. Nieto, “Analytical relations between kinetic-energy and particle densities for one-dimensional harmonically confined Fermi vapors,” *Phys. Rev. A* **63**, 044502 (2001).
- ⁵²P. Vignolo and A. Minguzzi, “Shell structure in the density profiles for noninteracting fermions in anisotropic harmonic confinement,” *Phys. Rev. A* **67**, 053601 (2003).
- ⁵³M. Brack and B. P. van Zyl, “Simple analytical particle and kinetic energy densities for a dilute fermionic gas in a d -dimensional harmonic trap,” *Phys. Rev. Lett.* **86**, 1574–1577 (2001).
- ⁵⁴D. S. Dean, P. Le Doussal, S. N. Majumdar, and G. Schehr, “Noninteracting fermions at finite temperature in a d -dimensional trap: Universal correlations,” *Phys. Rev. A* **94**, 063622 (2016).
- ⁵⁵J. Schneider and H. Wallis, “Mesoscopic Fermi gas in a harmonic trap,” *Phys. Rev. A* **57**, 1253–1259 (1998).
- ⁵⁶G. M. Bruun and K. Burnett, “Interacting Fermi gas in a harmonic trap,” *Phys. Rev. A* **58**, 2427–2434 (1998).
- ⁵⁷E. J. Mueller, “Density profile of a harmonically trapped ideal Fermi gas in arbitrary dimension,” *Phys. Rev. Lett.* **93**, 190404 (2004).
- ⁵⁸V. Dunjko, V. Lorent, and M. Olshanii, “Bosons in cigar-shaped traps: Thomas-Fermi regime, Tonks-Girardeau regime, and in between,” *Phys. Rev. Lett.* **86**, 5413–5416 (2001).
- ⁵⁹G. Lang, P. Vignolo, and A. Minguzzi, “Tan’s contact of a harmonically trapped one-dimensional Bose gas: Strong-coupling expansion and conjectural approach at arbitrary interactions,” *Eur. Phys. J. :ST* **226**, 1583–1891 (2017).
- ⁶⁰F. D. M. Haldane, “Effective harmonic-fluid approach to low-energy properties of one-dimensional quantum fluids,” *Phys. Rev. Lett.* **47**, 1840–1843 (1981).
- ⁶¹N. Didier, A. Minguzzi, and F. Hekking, “Generalized harmonic-fluid approach for the off-diagonal correlations of a one-dimensional interacting Bose gas,” *Phys. Rev. A* **80**, 033608 (2009).
- ⁶²A. Lenard, “—,” *J. Math. Phys.* **5**, 930 (1964).
- ⁶³H. G. Vaidya and C. A. Tracy, “One-particle reduced density matrix of impenetrable bosons in one dimension at zero temperature,” *Phys. Rev. Lett.* **42**, 3–6 (1979).
- ⁶⁴H. G. Vaidya and C. A. Tracy, “One-particle reduced density matrix of impenetrable bosons in one dimension at zero temperature,” *Phys. Rev. Lett.* **43**, 1540–1540 (1979).
- ⁶⁵M. Jimbo, T. Miwa, Y. Mori, and M. Sato, *Phys. D Nonlin. Phen.* **1**, 80 (1980).
- ⁶⁶D. M. Gangardt, “Universal correlations of trapped one-dimensional impenetrable bosons,” *Journal of Physics A: Mathematical and General* **37**, 9335–9356 (2004).
- ⁶⁷M. Olshanii and V. Dunjko, “Short-distance correlation properties of the lieb-liniger system and momentum distributions of trapped one-dimensional atomic gases,” *Phys. Rev. Lett.* **91**, 090401 (2003).
- ⁶⁸M. Olshanii, V. Dunjko, A. Minguzzi, and G. Lang, “Connection between nonlocal one-body and local three-body correlations of the lieb-liniger model,” *Phys. Rev. A* **96**, 033624 (2017).
- ⁶⁹R. Pezer and H. Buljan, “Momentum distribution dynamics of a Tonks-Girardeau gas: Bragg reflections of a quantum many-body wave packet,” *Phys. Rev. Lett.* **98**, 240403 (2007).
- ⁷⁰Y. Y. Atas, D. M. Gangardt, I. Bouchoule, and K. V. Kheruntsyan, “Exact nonequilibrium dynamics of finite-temperature Tonks-Girardeau gases,” *Phys. Rev. A* **95**, 043622 (2017).
- ⁷¹H. Cayla, C. Carcy, Q. Bouton, R. Chang, G. Carleo, M. Mancini, and D. Clément, “Single-atom-resolved probing of lattice gases in momentum space,” *Phys. Rev. A* **97**, 061609 (2018).
- ⁷²L. Mathey, A. Vishwanath, and E. Altman, “Noise correlations in low-dimensional systems of ultracold atoms,” *Phys. Rev. A* **79**, 013609 (2009).
- ⁷³K. He and M. Rigol, “Scaling of noise correlations in one-dimensional-lattice-hard-core-boson systems,” *Phys. Rev. A* **83**, 023611 (2011).
- ⁷⁴B. Fang, A. Johnson, T. Roscilde, and I. Bouchoule, “Momentum-space correlations of a one-dimensional Bose gas,” *Phys. Rev. Lett.* **116**, 050402 (2016).
- ⁷⁵I. Bouchoule, M. Arzamasovs, K. V. Kheruntsyan, and D. M. Gangardt, “Two-body momentum correlations in a weakly interacting one-dimensional Bose gas,” *Phys. Rev. A* **86**, 033626 (2012).
- ⁷⁶I. Lovas, B. Dóra, E. Demler, and G. Zaránd, “Full counting statistics of time-of-flight images,” *Phys. Rev. A* **95**, 053621 (2017).
- ⁷⁷P. Devillard, D. Chevallier, P. Vignolo, and M. Albert, “Full counting statistics of the momentum occupation numbers of the Tonks-Girardeau gas,” *Phys. Rev. A* **101**, 063604 (2020).
- ⁷⁸P. Devillard, A. Benzahi, P. Vignolo, and M. Albert, “Statistical properties of the momentum occupation numbers of the Tonks-Girardeau gas in a harmonic trap,” arXiv:2109.03493 (2021).
- ⁷⁹P. Vignolo, A. Minguzzi, and M. P. Tosi, “Light scattering from a degenerate quasi-one-dimensional confined gas of noninteracting fermions,” *Phys. Rev. A* **64**, 023421 (2001).
- ⁸⁰V. N. Golovach, A. Minguzzi, and L. I. Glazman, “Dynamic response of one-dimensional bosons in a trap,” *Phys. Rev. A* **80**, 043611 (2009).
- ⁸¹D. Clément, N. Fabbri, L. Fallani, C. Fort, and M. Inguscio, “Exploring correlated 1d Bose gases from the superfluid to the Mott-insulator state by inelastic light scattering,” *Phys. Rev. Lett.* **102**, 155301 (2009).
- ⁸²J. Decamp, J. Juenemann, M. Albert, M. Rizzi, A. Minguzzi, and P. Vignolo, “Strongly correlated one-dimensional Bose-Fermi quantum mixtures: symmetry and correlations,” *New Journal of Physics* **19**, 125001 (2017).
- ⁸³A. G. Volosniev, D. V. Fedorov, A. S. Jensen, N. T. Zinner, and M. Valiente, “Strongly interacting confined quantum systems in one dimension,” *Nature Communications* **5**, 5300 (2014).
- ⁸⁴F. Deuretzbacher, D. Becker, J. Bjerlin, S. Reimann, and L. Santos, “Quantum magnetism without lattices in strongly interacting one-dimensional spinor gases,” *Phys. Rev. A* **90**, 013611 (2014).
- ⁸⁵F. Deuretzbacher, K. Fredenhagen, D. Becker, K. Bongs, K. Sengstock, and D. Pfannkuche, “Exact solution of strongly interacting quasi-one-dimensional spinor Bose gases,” *Phys. Rev. Lett.* **100**, 160405 (2008).
- ⁸⁶B. Fang, P. Vignolo, M. Gattobigio, C. Miniatura, and A. Minguzzi, “Exact solution for the degenerate ground-state manifold of a strongly interacting one-dimensional Bose-Fermi mixture,” *Phys. Rev. A* **84**, 023626 (2011).
- ⁸⁷A. G. Volosniev, A. J. D. V. Fedorov, N. Zinner, and M. Valiente, “Multicomponent strongly interacting few-fermion systems in one dimension,” *Few-Body Systems* **55**, 839 (2014).

- ⁸⁸M. Ogata and H. Shiba, “Bethe-ansatz wave function, momentum distribution, and spin correlation in the one-dimensional strongly correlated Hubbard model,” *Phys. Rev. B* **41**, 2326–2338 (1990).
- ⁸⁹J. Decamp, J. Jünemann, M. Albert, M. Rizzi, A. Minguzzi, and P. Vignolo, “High-momentum tails as magnetic-structure probes for strongly correlated $SU(\kappa)$ fermionic mixtures in one-dimensional traps,” *Physical Review A* **94**, 053614 (2016).
- ⁹⁰X.-W. Guan, M. T. Batchelor, and C. Lee, “Fermi gases in one dimension: From Bethe ansatz to experiments,” *Rev. Mod. Phys.* **85**, 1633–1691 (2013).
- ⁹¹S. E. Gharashi and D. Blume, “Correlations of the upper branch of 1d harmonically trapped two-component Fermi gases,” *Phys. Rev. Lett.* **111**, 045302 (2013).
- ⁹²E. Lindgren, J. Rotureau, C. Forss, A. Volosniev, and N. Zinner, “Fermionization of two-component few-fermion systems in a one-dimensional harmonic trap,” *New J. Phys.* **16**, 063003 (2014).
- ⁹³R. E. Barfknecht, A. Foerster, and N. T. Zinner, “Dynamics of spin and density fluctuations in strongly interacting few-body systems,” *Sci. Rep.* **9**, 15994 (2019).
- ⁹⁴L. Yang, L. Guan, and H. Pu, “Strongly interacting quantum gases in one-dimensional traps,” *Phys. Rev. A* **91**, 043634 (2015).
- ⁹⁵L. Yang and X. Cui, “Effective spin-chain model for strongly interacting one-dimensional atomic gases with an arbitrary spin,” *Phys. Rev. A* **93**, 013617 (2016).
- ⁹⁶K. A. Matveev, “Conductance of a quantum wire at low electron density,” *Phys. Rev. B* **70**, 245319 (2004).
- ⁹⁷K. A. Matveev and A. Furusaki, “Spectral functions of strongly interacting isospin- $\frac{1}{2}$ bosons in one dimension,” *Phys. Rev. Lett.* **101**, 170403 (2008).
- ⁹⁸G. Pecci, P. Vignolo, and A. Minguzzi, “Universal scaling of spin mixing dynamics in a strongly interacting one-dimensional Fermi gas,” *arXiv:2107.12075* (2021).
- ⁹⁹G. James and A. Kerber, *The representation theory of the symmetric group* (Addison-Wesley, Reading, Massachusetts, 1981).
- ¹⁰⁰G. James and M. Liebeck, *Representations and Characters of Groups (2nd ed.)* (Cambridge University Press, Cambridge, London, 2001).
- ¹⁰¹J. Katriel, “Representation-free evaluation of the eigenvalues of the class-sums of the symmetric group,” *J. Phys. A* **26**, 135 (1993).
- ¹⁰²K. K. Das, M. D. Girardeau, and E. M. Wright, “Interference of a thermal Tonks gas on a ring,” *Phys. Rev. Lett.* **89**, 170404 (2002).
- ¹⁰³M. Cominotti, F. Hekking, and A. Minguzzi, “Dipole mode of a strongly correlated one-dimensional Bose gas in a split trap: Parity effect and barrier renormalization,” *Phys. Rev. A* **92**, 033628 (2015).
- ¹⁰⁴J. Polo, V. Ahufinger, F. W. J. Hekking, and A. Minguzzi, “Damping of Josephson oscillations in strongly correlated one-dimensional atomic gases,” *Phys. Rev. Lett.* **121**, 090404 (2018).
- ¹⁰⁵J. Polo, R. Dubessy, P. Pedri, H. Perrin, and A. Minguzzi, “Oscillations and decay of superfluid currents in a one-dimensional Bose gas on a ring,” *Phys. Rev. Lett.* **123**, 195301 (2019).
- ¹⁰⁶R. Dubessy, J. Polo, H. Perrin, A. Minguzzi, and M. Olshanii, “Universal shock-wave propagation in one-dimensional Bose fluids,” *Phys. Rev. Research* **3**, 013098 (2021).
- ¹⁰⁷P. Capuzzi and P. Vignolo, “Finite-temperature contact for a $su(2)$ Fermi gas trapped in a one-dimensional harmonic confinement,” *Phys. Rev. A* **101**, 013633 (2020).
- ¹⁰⁸A. Lenard, “One-dimensional impenetrable bosons in thermal equilibrium,” *Journal of Mathematical Physics* **7**, 1268–1272 (1966), <https://doi.org/10.1063/1.1705029>.
- ¹⁰⁹P. Vignolo and A. Minguzzi, “Universal contact for a Tonks-Girardeau gas at finite temperature,” *Phys. Rev. Lett.* **110**, 020403 (2013).
- ¹¹⁰A. Lenard, “Momentum distribution in the ground state of the one-dimensional system of impenetrable bosons,” *Journal of Mathematical Physics* **5**, 930–943 (1964), <https://doi.org/10.1063/1.1704196>.
- ¹¹¹J. Gould and T. Busch, “Ground-state properties of a Tonks-Girardeau gas in a split trap,” *Phys. Rev. A* **77**, 063601 (2008).
- ¹¹²M. A. Cazalilla, “Bosonizing one-dimensional cold atomic gases,” *Journal of Physics B* **37**, S1–S47 (2004).
- ¹¹³A. Colcelli, G. Mussardo, and A. Trombettoni, “Deviations from off-diagonal long-range order in one-dimensional quantum systems,” *EPL (Europhysics Letters)* **122**, 50006 (2018).
- ¹¹⁴M. A. Cazalilla, *J. Phys. B* **37**, S1 (2003).
- ¹¹⁵A. Minguzzi, P. Vignolo, and M. P. Tosi, “High momentum tail in the Tonks gas under harmonic confinement,” *Phys. Lett. A* **294**, 222 (2002).
- ¹¹⁶S. Tan, “Large momentum part of fermions with large scattering length,” *Ann. Phys. (N.Y.)* **323**, 2971 (2008).
- ¹¹⁷S. Tan, “Generalized virial theorem and pressure relation for a strongly correlated Fermi gas,” *Ann. Phys. (N.Y.)* **323**, 2987 (2008).
- ¹¹⁸S. Tan, “Energetics of a strongly correlated Fermi gas,” *Ann. Phys. (N.Y.)* **323**, 2952 (2008).
- ¹¹⁹M. Barth and W. Zwerger, “Tan relations in one dimension,” *Annals of Physics* **326**, 2544 (2011).
- ¹²⁰B. Y. Fang, P. Vignolo, C. Miniatura, and A. Minguzzi, “Fermionization of a strongly interacting Bose-Fermi mixture in a one-dimensional harmonic trap,” *Phys. Rev. A* **79**, 023623 (2009).
- ¹²¹F. T. Sant’Ana, F. Hébert, V. G. Rousseau, M. Albert, and P. Vignolo, “Scaling properties of tan’s contact: Embedding pairs and correlation effect in the Tonks-Girardeau limit,” *Phys. Rev. A* **100**, 063608 (2019).
- ¹²²G. Lang, F. Hekking, and A. Minguzzi, “Ground-state energy and excitation spectrum of the Lieb-Liniger model: accurate analytical results and conjectures about the exact solution,” *SciPost Phys.* **3**, 003 (2017).
- ¹²³N. J. S. Loft, L. B. Kristensen, A. E. Thomsen, and N. T. Zinner, *Journal of Physics B* **49**, 125305 (2016).
- ¹²⁴C. N. Yang and C. P. Yang, “Thermodynamics of a one-dimensional system of bosons with repulsive delta-function interaction,” *Journal of Mathematical Physics* **10**, 1115–1122 (1969), <https://doi.org/10.1063/1.1664947>.
- ¹²⁵O. I. Pâtu and A. Klümper, “Thermodynamics, contact, and density profiles of the repulsive gaudin-yang model,” *Phys. Rev. A* **93**, 033616 (2016).
- ¹²⁶O. I. Pâtu, A. Klümper, and A. Foerster, “Universality and quantum criticality of the one-dimensional spinor Bose gas,” *Phys. Rev. Lett.* **120**, 243402 (2018).
- ¹²⁷H. Yao, D. Clément, A. Minguzzi, P. Vignolo, and L. Sanchez-Palencia, “Tan’s contact for trapped lieb-liniger bosons at finite temperature,” *Phys. Rev. Lett.* **121**, 220402 (2018).
- ¹²⁸M. Rizzi, C. Miniatura, A. Minguzzi, and P. Vignolo, “Scaling behavior of tan’s contact for trapped lieb-liniger bosons: From two to many,” *Phys. Rev. A* **98**, 043607 (2018).
- ¹²⁹P. Vignolo, A. Minguzzi, and M. P. Tosi, “Exact particle and kinetic energy density for one-dimensional confined gases of non-interacting fermions,” *Phys. Rev. Lett.* **85**, 2850 (2000).
- ¹³⁰F. Deuretzbacher, D. Becker, and L. Santos, “Momentum distributions and numerical methods for strongly interacting one-dimensional spinor gases,” *Phys. Rev. A* **94**, 023606 (2016).
- ¹³¹J. Decamp, P. Armagnat, B. Fang, M. Albert, A. Minguzzi, and P. Vignolo, “Exact density profiles and symmetry classification for strongly interacting multi-component Fermi gases in tight waveguides,” *New Journal of Physics* **18**, 055011 (2016).
- ¹³²H. Hu, L. Guan, and S. Chen, “Strongly interacting Bose-Fermi mixtures in one dimension,” *New Journal of Physics* **18**, 025009 (2016).
- ¹³³A. S. Dehkharghani, F. F. Bellotti, and N. T. Zinner, “Analytical and numerical studies of Bose-Fermi mixtures in a one-dimensional harmonic trap,” *J. of Phys. B: At. Mol. Opt. Phys.* **50**, 144002 (2017).
- ¹³⁴A. S. Dehkharghani, F. F. Bellotti, and N. T. Zinner, “Analytical and numerical studies of Bose-Fermi mixtures in a one-dimensional harmonic trap,” *Journal of Physics B: Atomic, Molecular and Optical Physics* **50**, 144002 (2017).
- ¹³⁵A. Imambekov and E. Demler, “Applications of exact solution for strongly interacting one-dimensional Bose-Fermi mixture: Low-temperature correlation functions, density profiles, and collective modes,” *Annals of Physics* **321**, 2390 – 2437 (2006).
- ¹³⁶A. Imambekov and L. I. Glazman, *Phys. Rev. Lett.* **102**, 126405 (2009).
- ¹³⁷G. Lang, F. Hekking, and A. Minguzzi, “Dynamic structure factor and drag force in a one-dimensional strongly interacting Bose gas at finite temperature,” *Phys. Rev. A* **91**, 063619 (2015).
- ¹³⁸J. De Nardis and M. Panfil, “Edge singularities and quasilong-range order in nonequilibrium steady states,” *Phys. Rev. Lett.* **120**, 217206 (2018).
- ¹³⁹K. Bencheikh, L. M. Nieto, and L. U. Ancarani, “The momentum distribution of two bosons in one dimension with infinite contact repulsion in harmonic trap gets analytical,” *arXiv:2104.06693* (2021).
- ¹⁴⁰A. Dehkharghani, A. Volosniev, J. Lindgren, J. Rotureau, C. Forssén, D. Fedorov, A. Jensen, and N. Zinner, “Quantum magnetism in strongly interacting one-dimensional spinor Bose systems,” *Scientific Reports* **5**,

- 10675 (2015).
- ¹⁴¹A. S. Dehkharghani, A. G. Volosniev, and N. T. Zinner, “Quantum impurity in a one-dimensional trapped Bose gas,” *Phys. Rev. A* **92**, 031601 (2015).
- ¹⁴²V. V. Cheianov, H. Smith, and M. B. Zvonarev, “Low-temperature crossover in the momentum distribution of cold atomic gases in one dimension,” *Phys. Rev. A* **71**, 033610 (2005).
- ¹⁴³M. Rigol and A. Muramatsu, “Ground-state properties of hard-core bosons confined on one-dimensional optical lattices,” *Phys. Rev. A* **72**, 013604 (2005).
- ¹⁴⁴M. Collura, S. Sotiriadis, and P. Calabrese, “Equilibration of a Tonks-Girardeau gas following a trap release,” *Phys. Rev. Lett.* **110**, 245301 (2013).
- ¹⁴⁵M. Collura, S. Sotiriadis, and P. Calabrese, “Quench dynamics of a Tonks-Girardeau gas released from a harmonic trap,” *Journal of Statistical Mechanics: Theory and Experiment* **2013**, P09025 (2013).
- ¹⁴⁶Y. Y. Atas, I. Bouchoule, D. M. Gangardt, and K. V. Kheruntsyan, “Collective many-body bounce in the breathing-mode oscillations of a Tonks-Girardeau gas,” *Phys. Rev. A* **96**, 041605 (2017).
- ¹⁴⁷B. Fang, G. Carleo, A. Johnson, and I. Bouchoule, “Quench-induced breathing mode of one-dimensional Bose gases,” *Phys. Rev. Lett.* **113**, 035301 (2014).
- ¹⁴⁸O. A. Castro-Alvaredo, B. Doyon, and T. Yoshimura, “Emergent hydrodynamics in integrable quantum systems out of equilibrium,” *Phys. Rev. X* **6**, 041065 (2016).
- ¹⁴⁹B. Bertini, M. Collura, J. De Nardis, and M. Fagotti, “Transport in out-of-equilibrium xxz chains: Exact profiles of charges and currents,” *Phys. Rev. Lett.* **117**, 207201 (2016).
- ¹⁵⁰A. del Campo and J. G. Muga, “Dynamics of a Tonks-Girardeau gas released from a hard-wall trap,” *Europhysics Letters (EPL)* **74**, 965–971 (2006).
- ¹⁵¹T. Fogarty and T. Busch, “A many-body heat engine at criticality,” *Quantum Science and Technology* **6**, 015003 (2020).
- ¹⁵²J. Goold, M. Krych, Z. Idziaszek, T. Fogarty, and T. Busch, “An eccentrically perturbed Tonks-Girardeau gas,” *New Journal of Physics* **12**, 093041 (2010).
- ¹⁵³B. Damski, “Shock waves in ultracold Fermi (Tonks) gases,” *Journal of Physics B: Atomic, Molecular and Optical Physics* **37**, L85–L91 (2004).
- ¹⁵⁴S. A. Simmons, F. A. Bayocboc, J. C. Pillay, D. Colas, I. P. McCulloch, and K. V. Kheruntsyan, “What is a quantum shock wave?” *Phys. Rev. Lett.* **125**, 180401 (2020).
- ¹⁵⁵L. Rutherford, J. Goold, T. Busch, and J. F. McCann, “Transport, atom blockade, and output coupling in a Tonks-Girardeau gas,” *Phys. Rev. A* **83**, 055601 (2011).
- ¹⁵⁶F. Cartarius, E. Kawasaki, and A. Minguzzi, “Dynamical depinning of a Tonks-Girardeau gas,” *Phys. Rev. A* **92**, 063605 (2015).
- ¹⁵⁷M. Mikkelsen, T. Fogarty, and T. Busch, “Static and dynamic phases of a Tonks-Girardeau gas in an optical lattice,” *New Journal of Physics* **20**, 113011 (2018).
- ¹⁵⁸M. Ljubotina, M. Žnidarič, and T. Prosen, “Spin diffusion from an inhomogeneous quench in an integrable system,” *Nature communications* **8**, 1–6 (2017).
- ¹⁵⁹D. Wei, A. Rubio-Abadal, B. Ye, F. Machado, J. Kemp, K. Srakaew, S. Hollerith, J. Rui, S. Gopalakrishnan, N. Y. Yao, I. Bloch, and J. Zeiher, “Quantum gas microscopy of kardar-parisi-zhang superdiffusion,” (2021), arXiv:2107.00038 [cond-mat.quant-gas].
- ¹⁶⁰Z. Akdeniz, P. Vignolo, A. Minguzzi, and M. P. Tosi, “Temperature dependence of density profiles for a cloud of noninteracting fermions moving inside a harmonic trap in one dimension,” *Phys. Rev. A* **66**, 055601 (2002).
- ¹⁶¹F. Deuretzbacher and L. Santos, “Tuning an effective spin chain of three strongly interacting one-dimensional fermions with the transversal confinement,” *Phys. Rev. A* **96**, 013629 (2017).
- ¹⁶²F. Deuretzbacher, D. Becker, J. Bjerlin, S. M. Reimann, and L. Santos, “Spin-chain model for strongly interacting one-dimensional Bose-Fermi mixtures,” *Phys. Rev. A* **95**, 043630 (2017).
- ¹⁶³N. Didier, A. Minguzzi, and F. W. J. Hekking, “Quantum fluctuations of a Bose-Josephson junction in a quasi-one-dimensional ring trap,” *Phys. Rev. A* **79**, 063633 (2009).
- ¹⁶⁴A. Imambekov, T. L. Schmidt, and L. I. Glazman, “One-dimensional quantum liquids: Beyond the luttinger liquid paradigm,” *Rev. Mod. Phys.* **84**, 1253–1306 (2012).
- ¹⁶⁵M. Rigol, V. Dunjko, and M. Olshanii, “Thermalization and its mechanism for generic isolated quantum systems,” *Nature* **452**, 854–858 (2008).
- ¹⁶⁶M. Ljubotina, M. Žnidarič, and T. c. v. Prosen, “Kardar-parisi-zhang physics in the quantum Heisenberg magnet,” *Phys. Rev. Lett.* **122**, 210602 (2019).
- ¹⁶⁷M. Kardar, G. Parisi, and Y.-C. Zhang, “Dynamic scaling of growing interfaces,” *Phys. Rev. Lett.* **56**, 889–892 (1986).
- ¹⁶⁸N. Loft, L. Kristensen, A. Thomsen, A. Volosniev, and N. Zinner, “Conan—the cruncher of local exchange coefficients for strongly interacting confined systems in one dimension,” *Computer Physics Communications* **209**, 171–182 (2016).
- ¹⁶⁹R. E. Barfknecht, A. Foerster, N. T. Zinner, and A. G. Volosniev, “Generation of spin currents by a temperature gradient in a two-terminal device,” (2021), arXiv:2101.02020 [cond-mat.quant-gas].
- ¹⁷⁰N. Loft, A. Dehkharghani, N. Mehta, and et al., “A variational approach to repulsively interacting three-fermion systems in a one-dimensional harmonic trap,” *Eur. Phys. J. D* **69**, 65 (2015).
- ¹⁷¹A. S. Dehkharghani, A. G. Volosniev, and N. T. Zinner, “Impenetrable mass-imbalanced particles in one-dimensional harmonic traps,” *Journal of Physics B* **49**, 085301 (2016).
- ¹⁷²T. Scoquart, J. J. Seaward, S. G. Jackson, and M. Olshanii, “Exactly solvable quantum few-body systems associated with the symmetries of the three-dimensional and four-dimensional icosahedra,” *SciPost Phys.* **1**, 005 (2016).
- ¹⁷³N. L. Harshman, M. Olshanii, A. S. Dehkharghani, A. G. Volosniev, S. G. Jackson, and N. T. Zinner, “Integrable families of hard-core particles with unequal masses in a one-dimensional harmonic trap,” *Phys. Rev. X* **7**, 041001 (2017).